Anisotropic RTM applied to field data

Philipp Witte, Felix J. Herrmann, October 26, 2015

SLIM
University of British Columbia

Introduction

Seismic survey by BP from Machar oil field

- initial 3D marine survey in eastern North Sea in 1989
- high density OBC multi-azimuth survey in 2011
- large salt dome with chalk and sandstone oil reservoirs

Seismic imaging and processing by BP

- difficult conditions due to weak reservoir reflectivity, multiples and disruption from shallow gas channels
- post-stack time migration image in 1990
- pre-stack time migration in 2003
- anisotropic pre-stack Kirchhoff migration in 2006

 (Ward et al., 2012, The Machar Oil Field, UK Central North Sea: impact of seismic reprocessing on the development of a complex fractured chalk field)

Introduction

BP supplied us with a 2D line from the 2011 OBC data set

- 330 Shots with 8 seconds recording time (50 m shot spacing)
- up to 505 receivers (25 m spacing)
- background velocity model + anisotropy parameters
- particular interest in eastern flank of salt dome

The shots were preprocessed by BP

- source designature
- mute of direct wave
- removal of multiples

Shot record

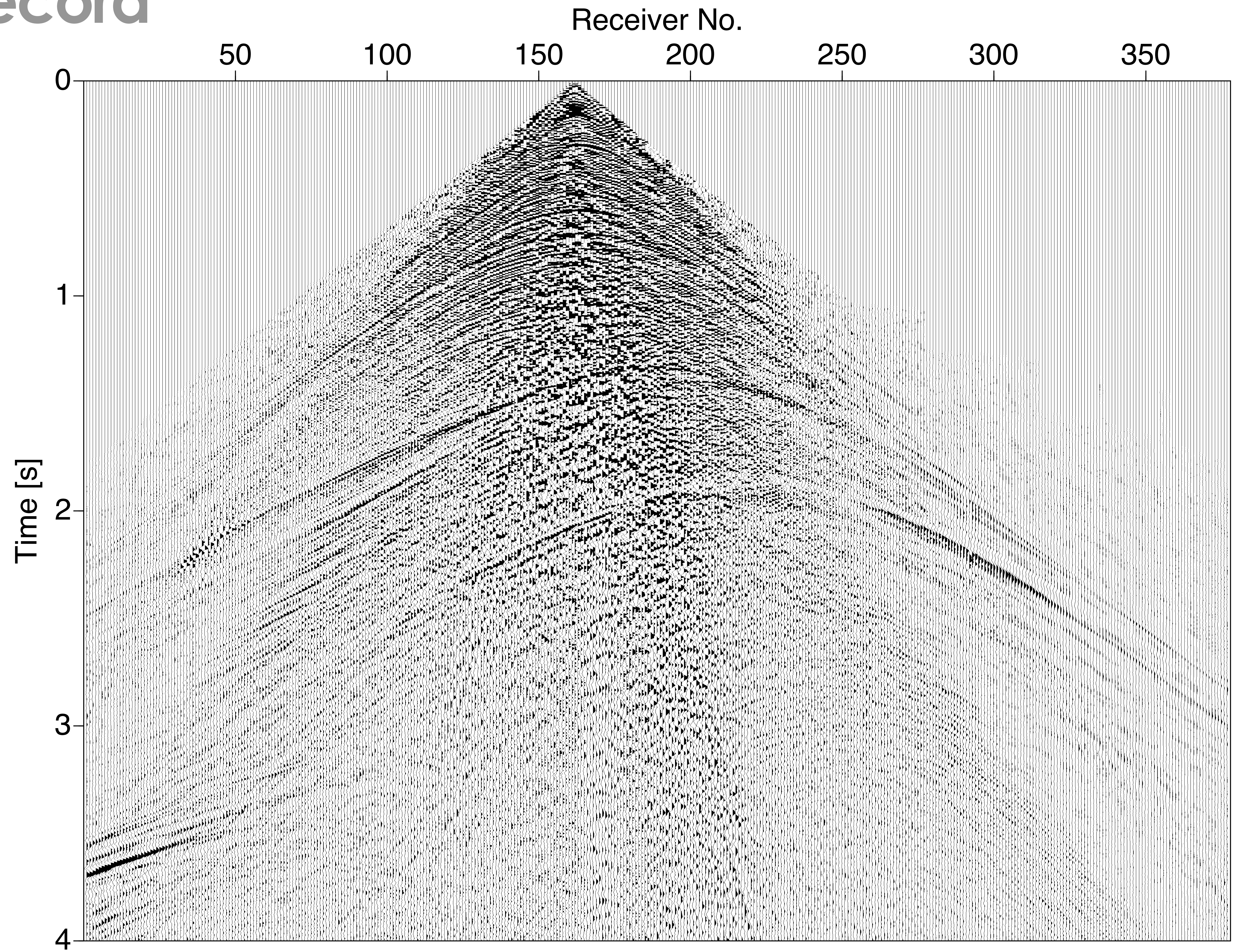

(All shown data and subsurface parameters by courtesy of BP)

FK Spectra

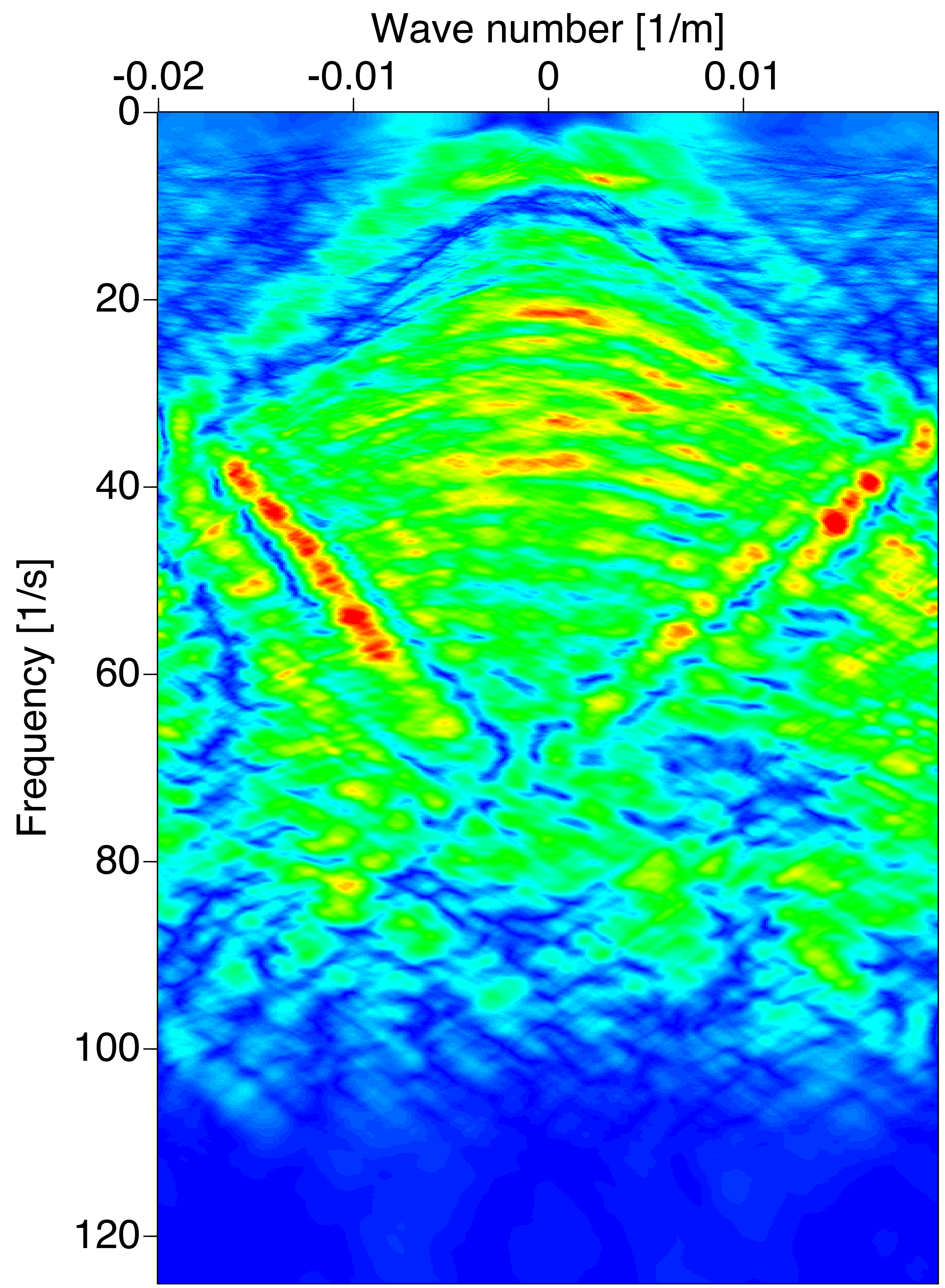

Shot No. 80

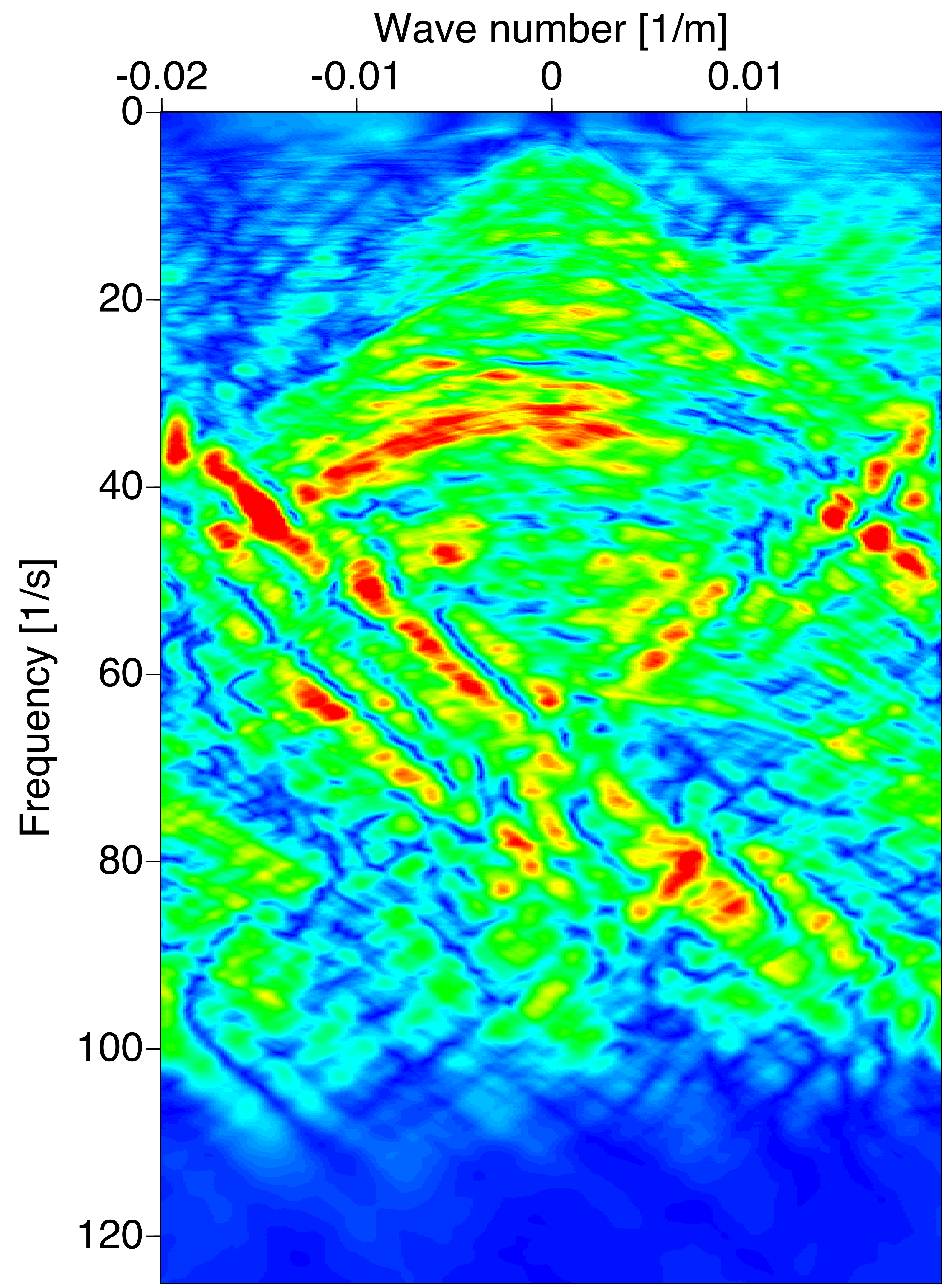

Shot No. 120

FK Spectra

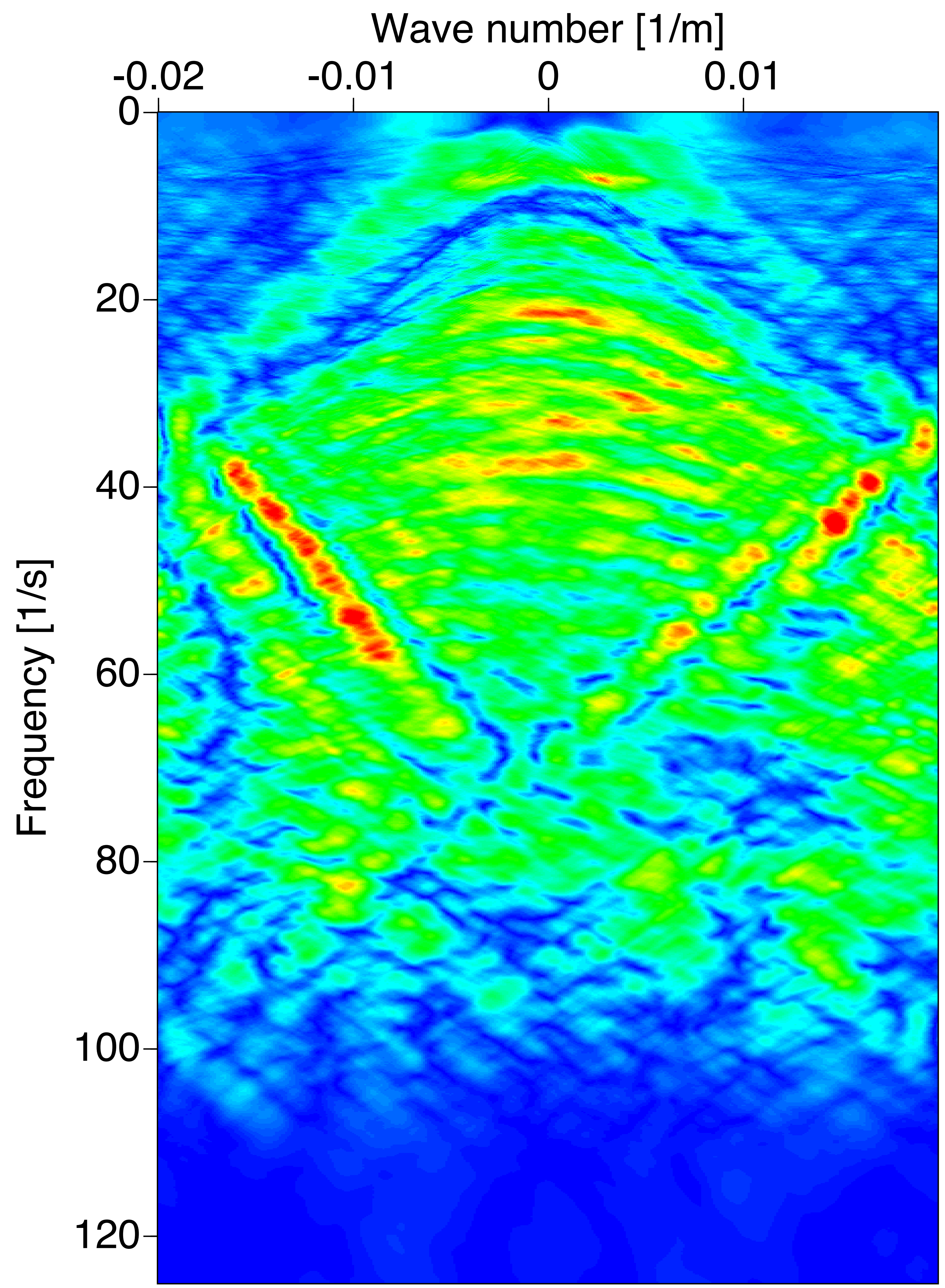

Shot No. 80

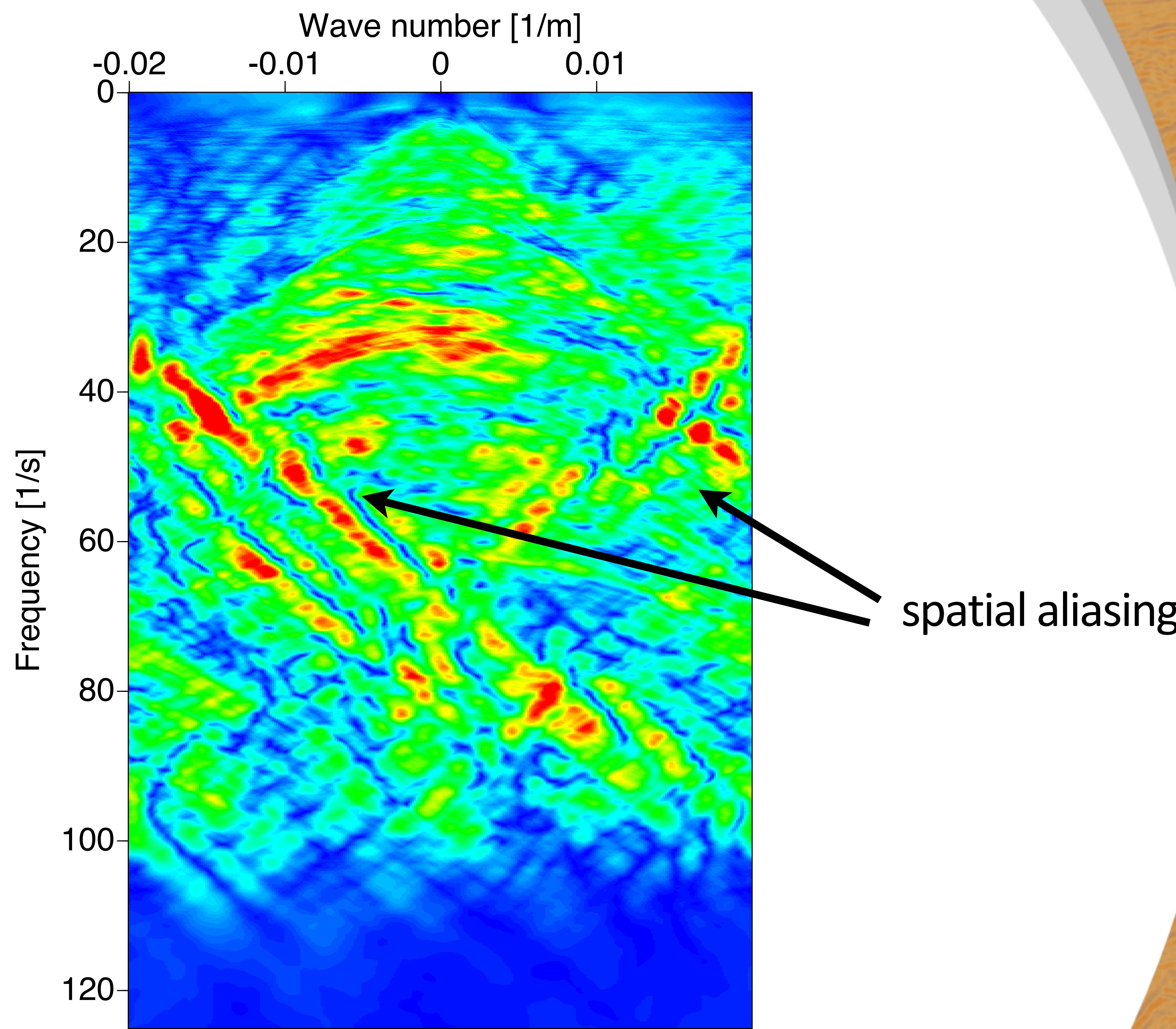

Shot No. 120

Machar velocity model

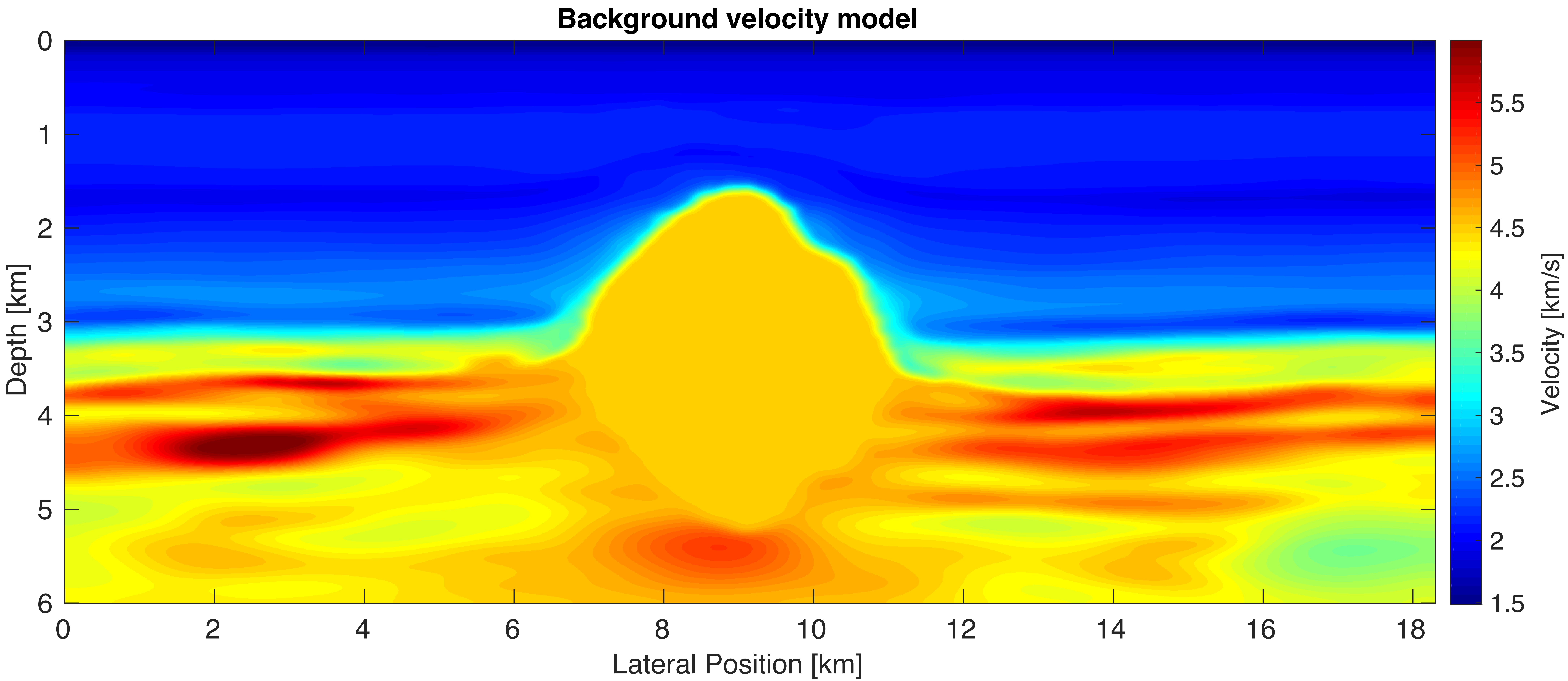

RTM Image

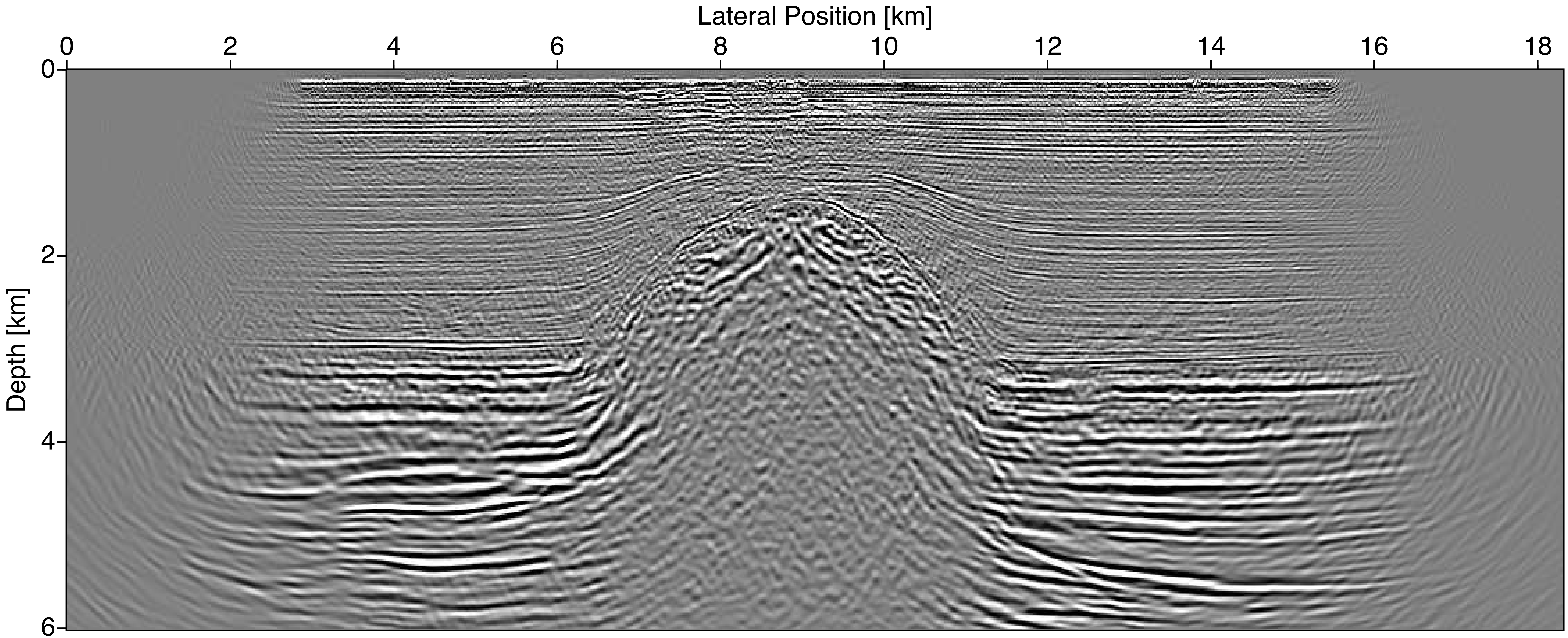

Result with data supplied by BP

Close-Up

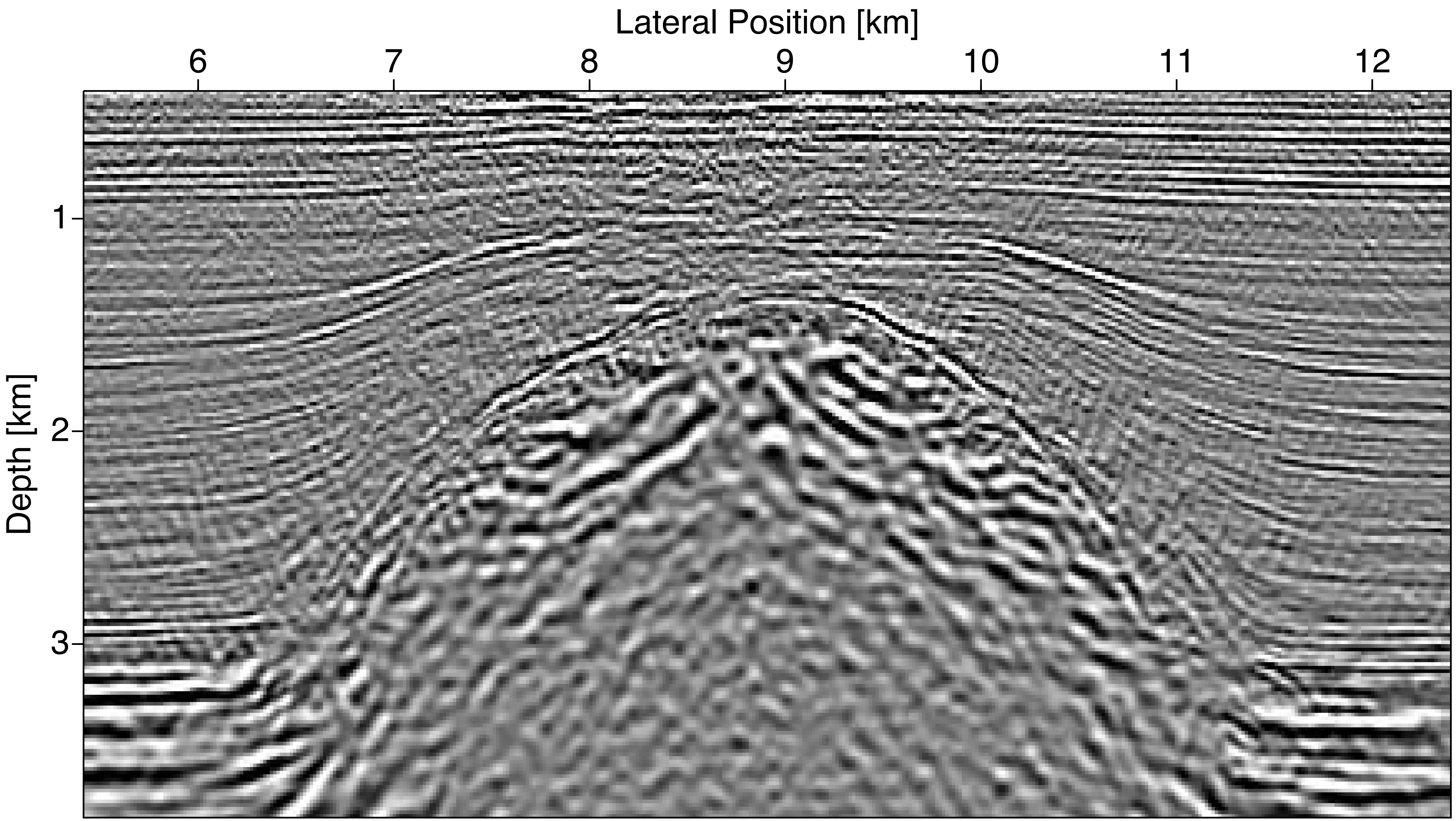

Machar data set

Initial shot records:

- spatial aliasing
- noise/marine ground roll
- corrupted traces

SLIM preprocessing:

- trace interpolation via curvelet-domain basis pursuit
- FK filtering

(Ning Tu, Tim Lin, Zhilong Fang (2013): Slim's findings on the Machar data set)

Shot record

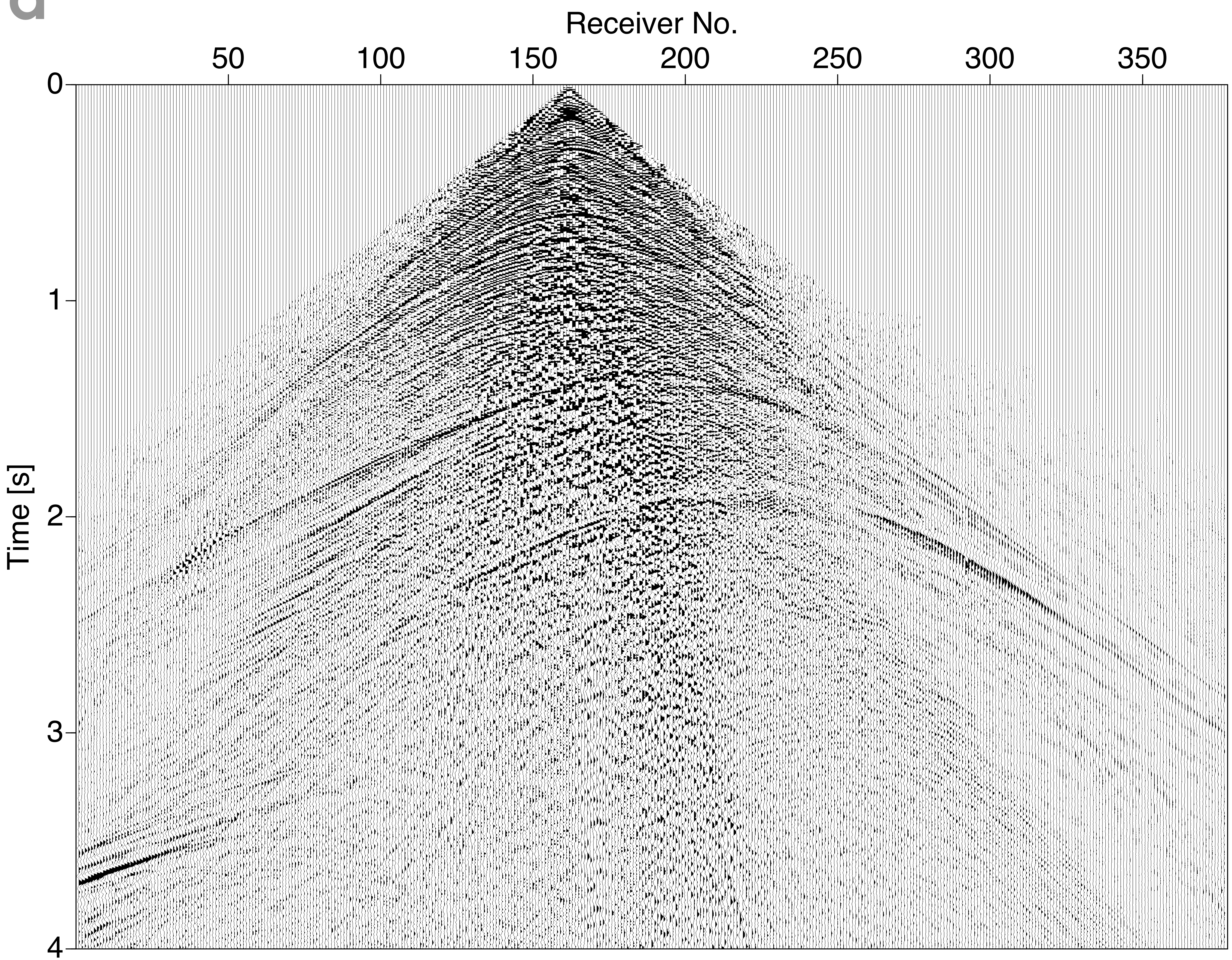

Initial shot record

Shot record

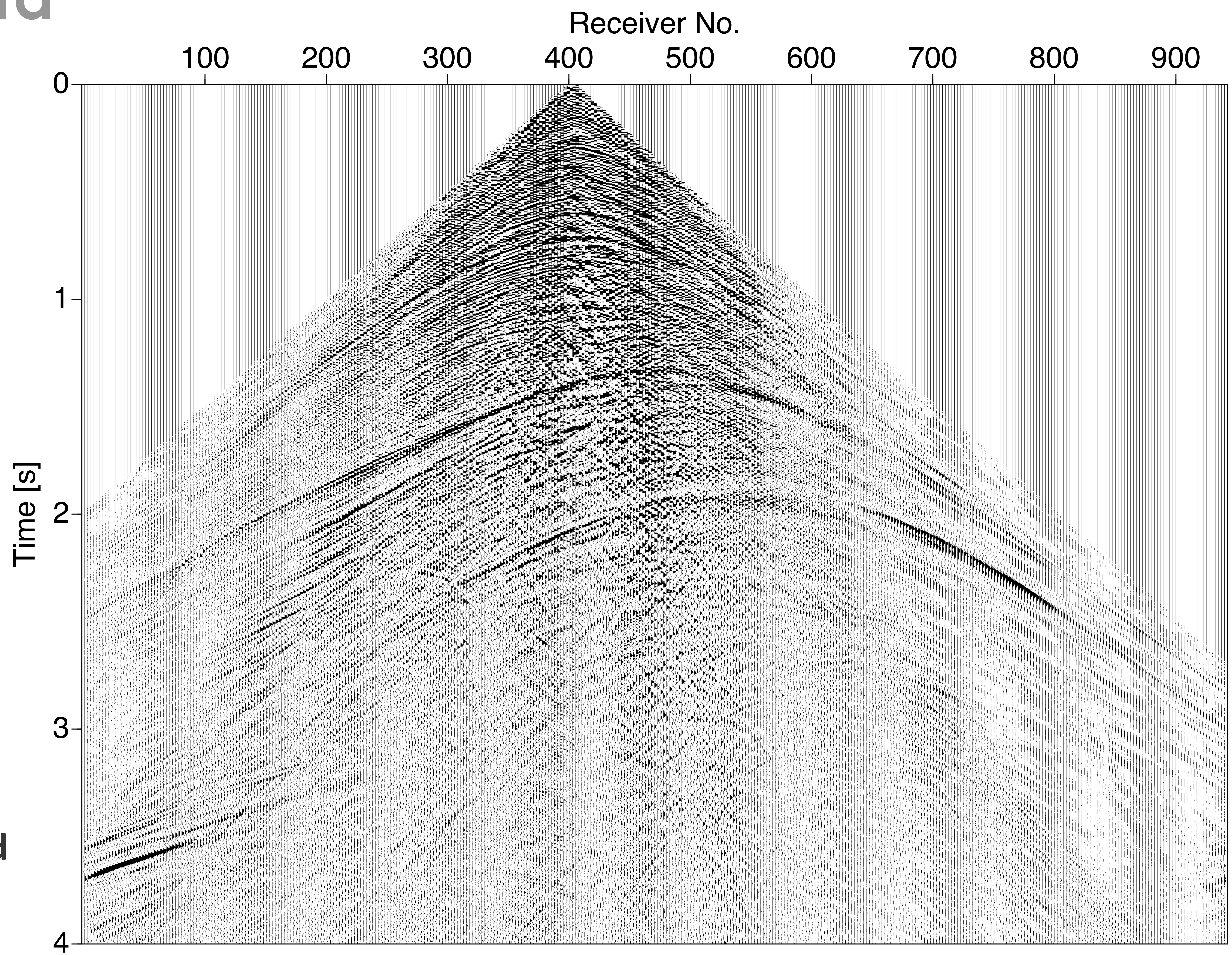

Processed shot record

FK Spectra

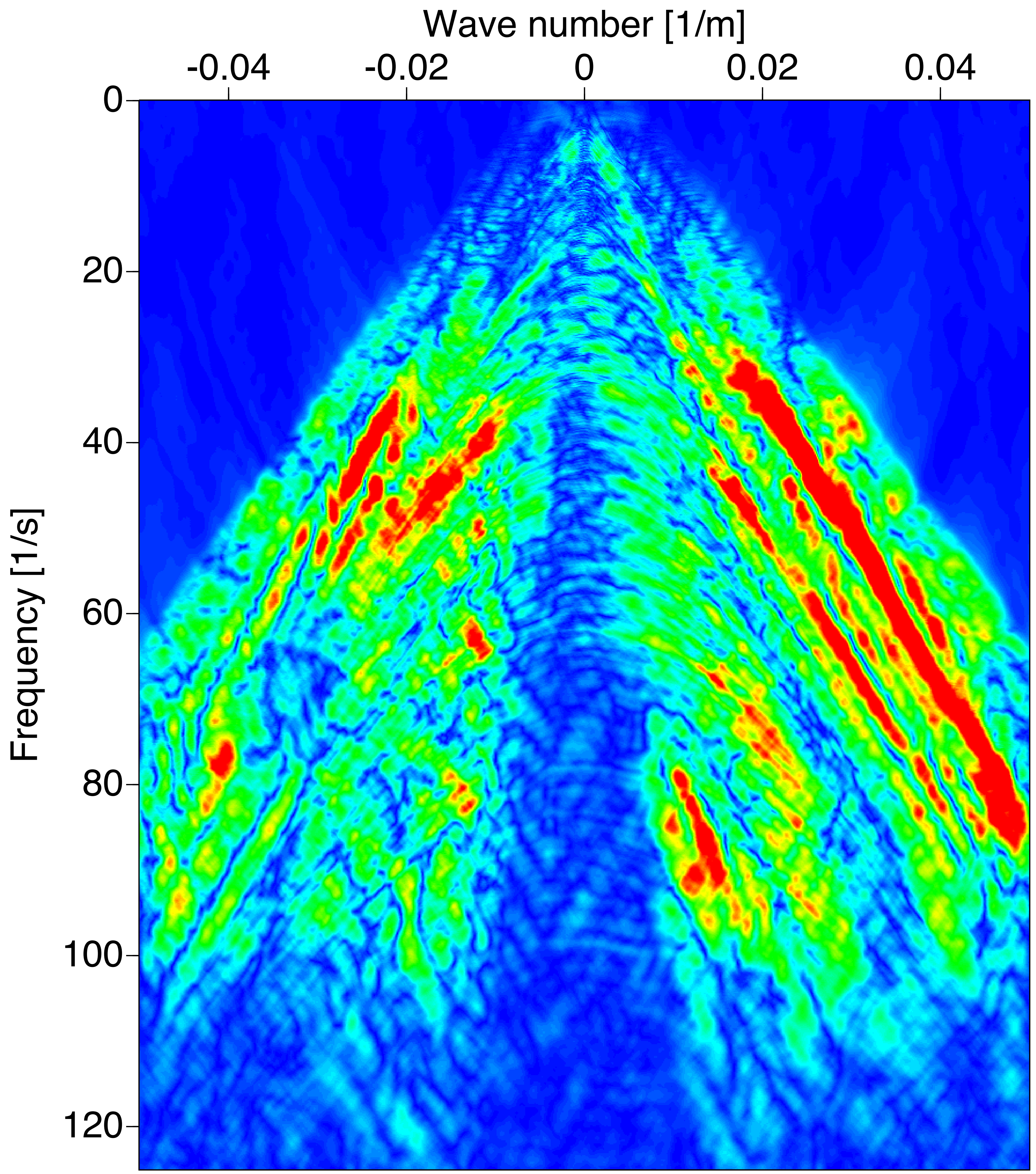

Shot No. 80

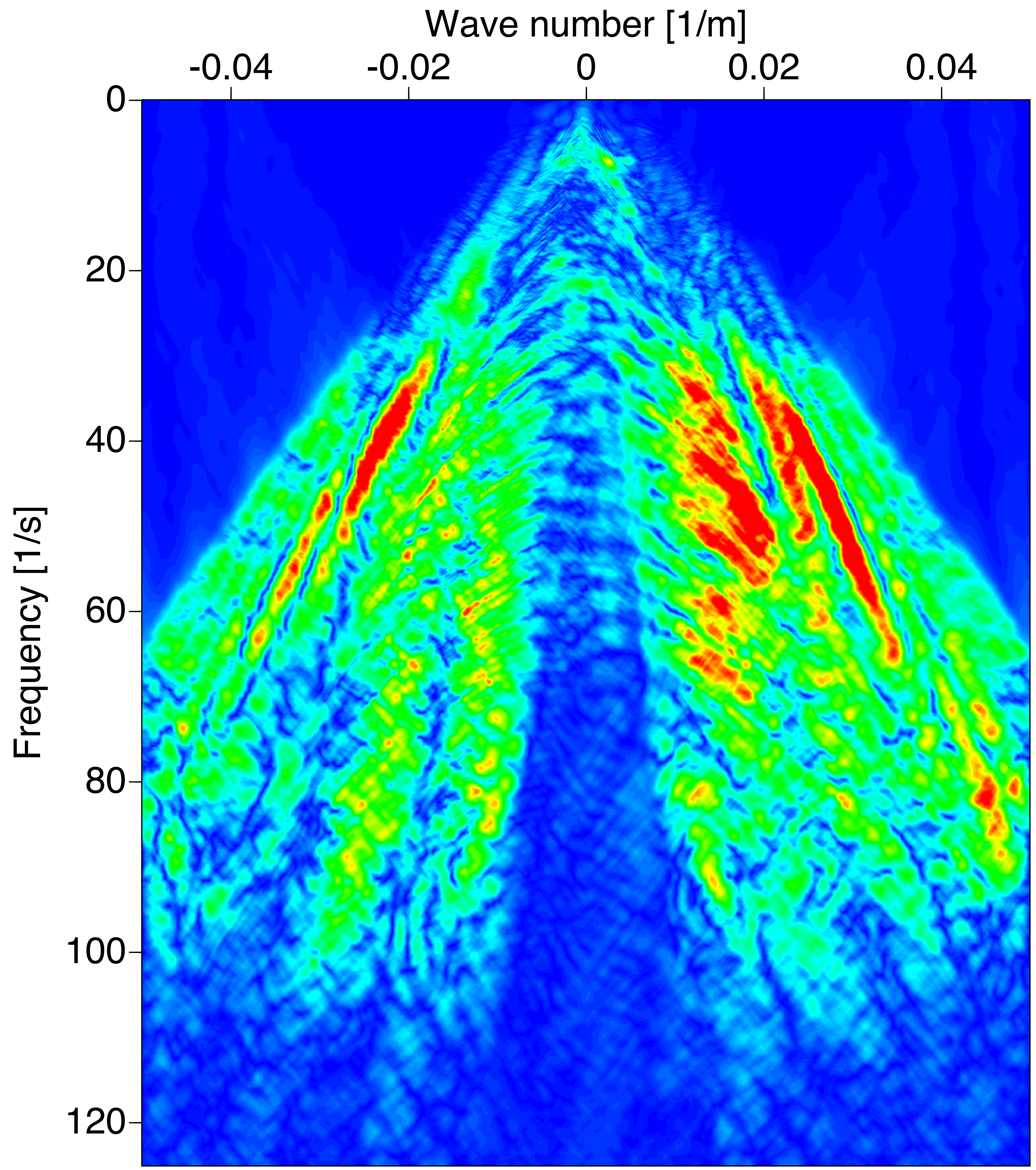

Shot No. 120

RTM Image

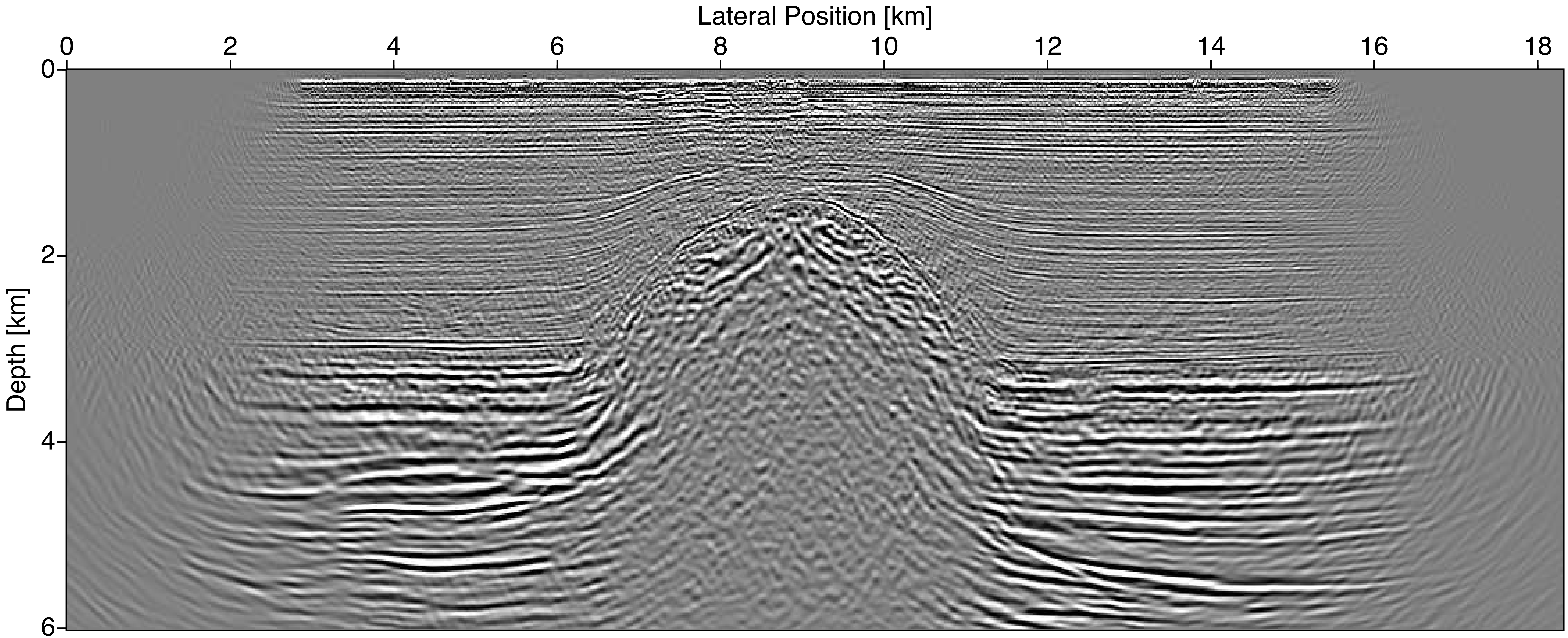

Result with data supplied by BP

RTM Image

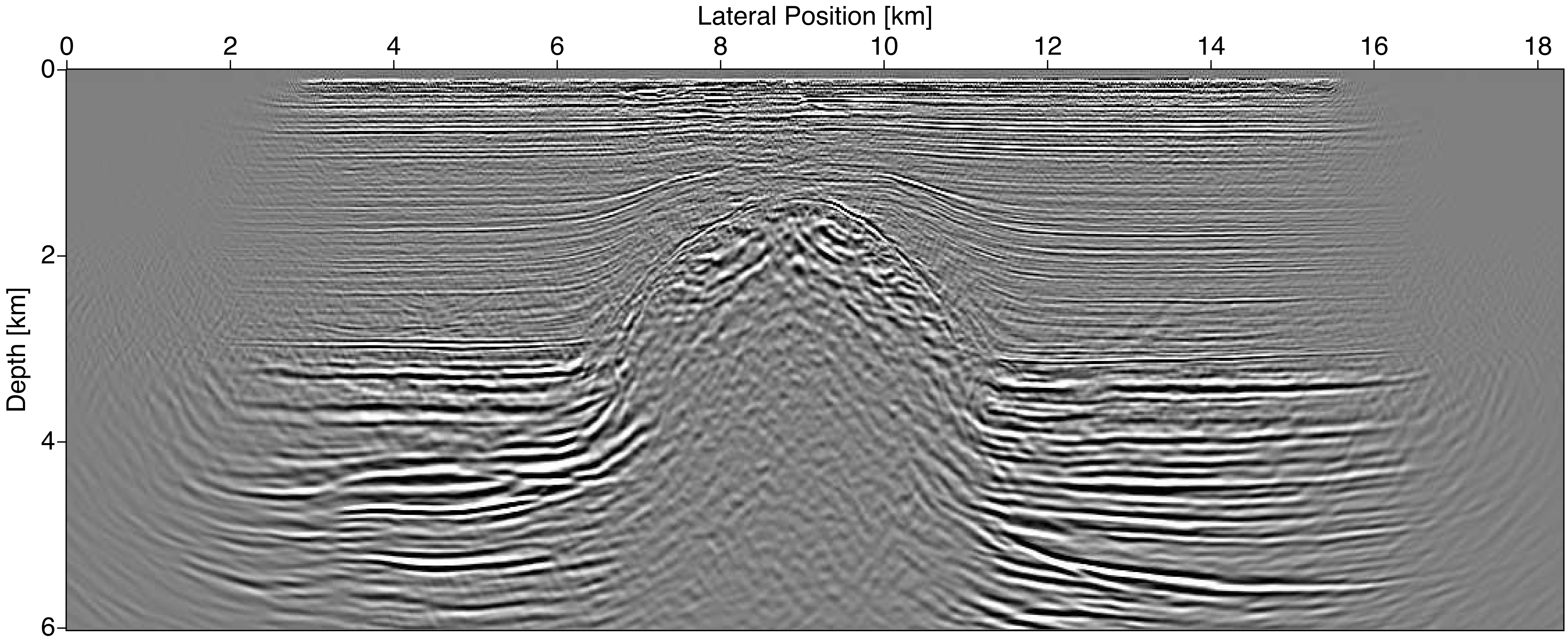

Result with processed data

Close-Up

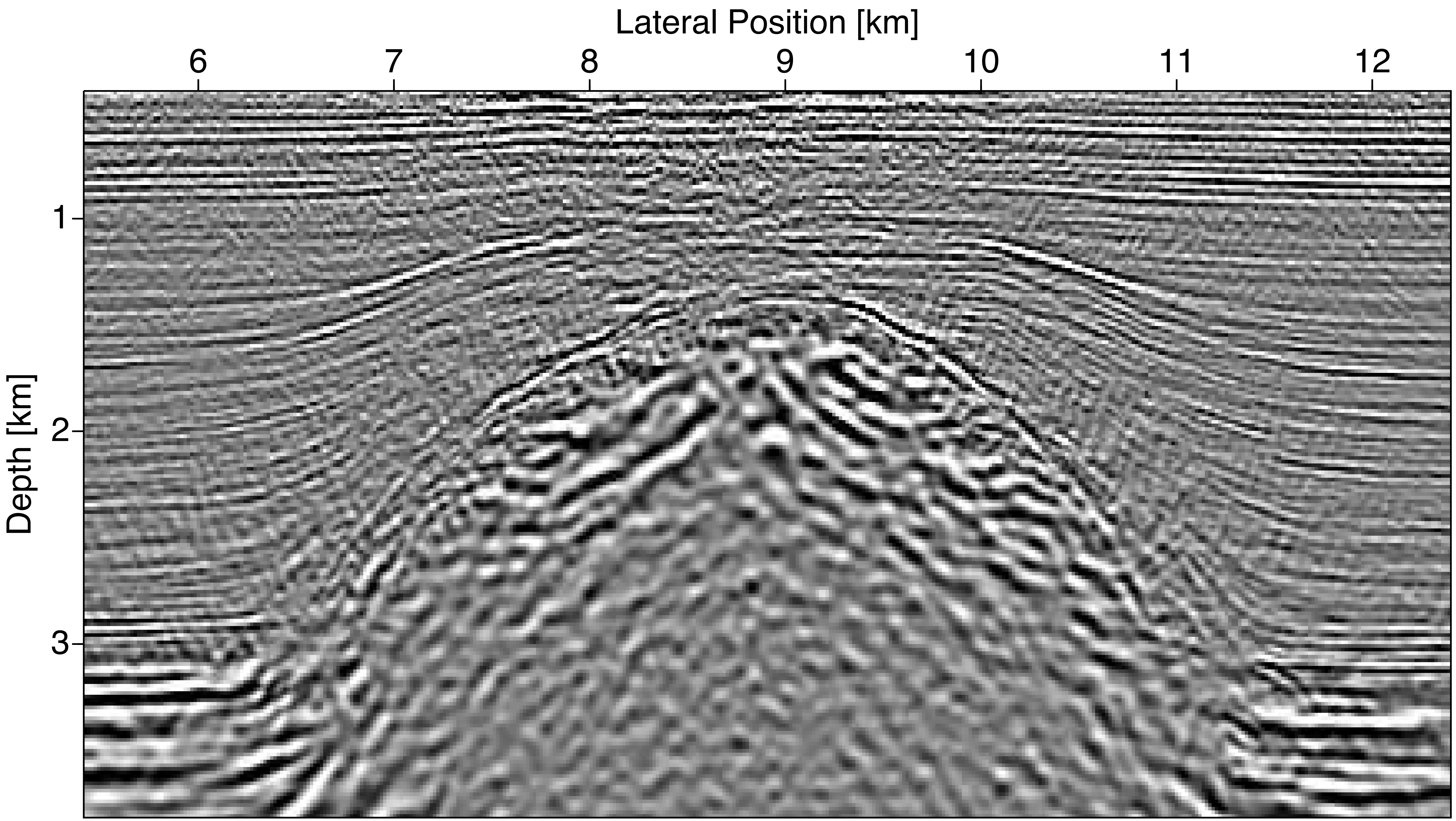

Result with data supplied by BP

Close-Up

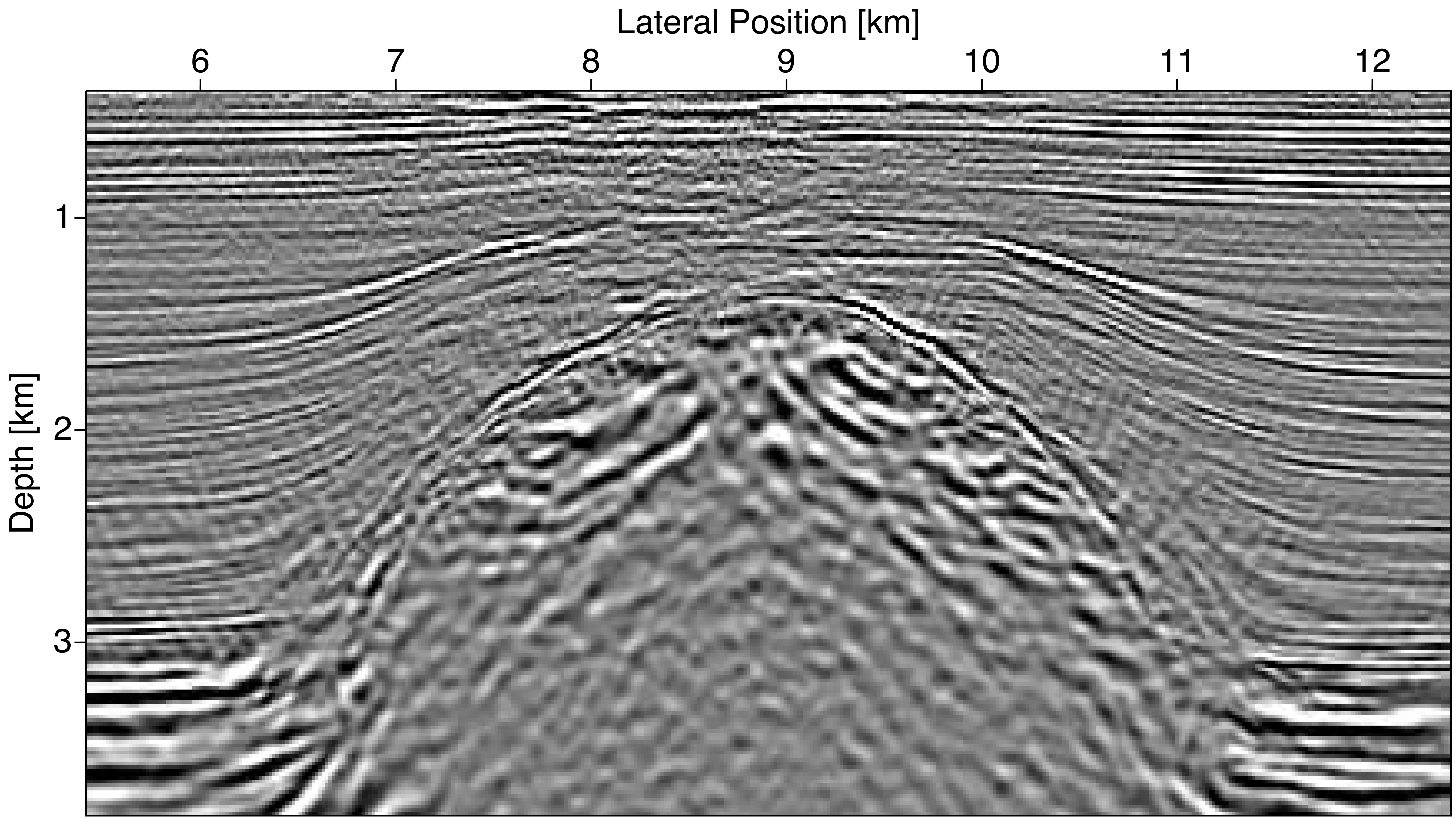

Result with processed data

RTM

RTM image still has low quality

- many reflectors discontinuous
- salt dome flanks poorly imaged
- low seismic coherence on eastern part of the flank

So far: imaging with acoustic wave equation

- migration with vertical velocity
- anisotropy not accounted for

Anisotropy – Thomson Parameters

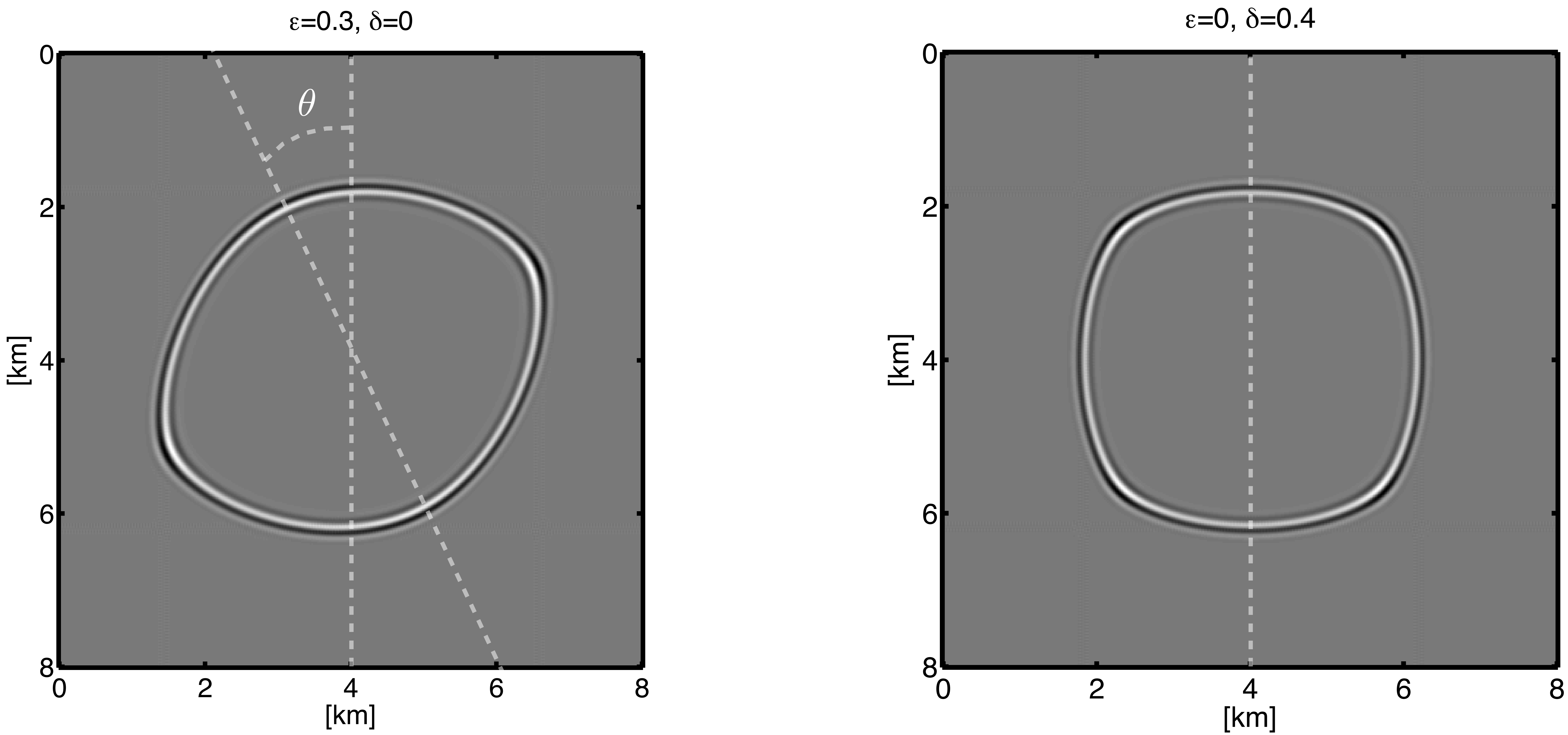

$$v_{p_x} = v_{p_z}\sqrt{1+2\epsilon}$$

$$v_{p_n} = v_{p_z}\sqrt{1+2\delta}$$

Machar: model parameters

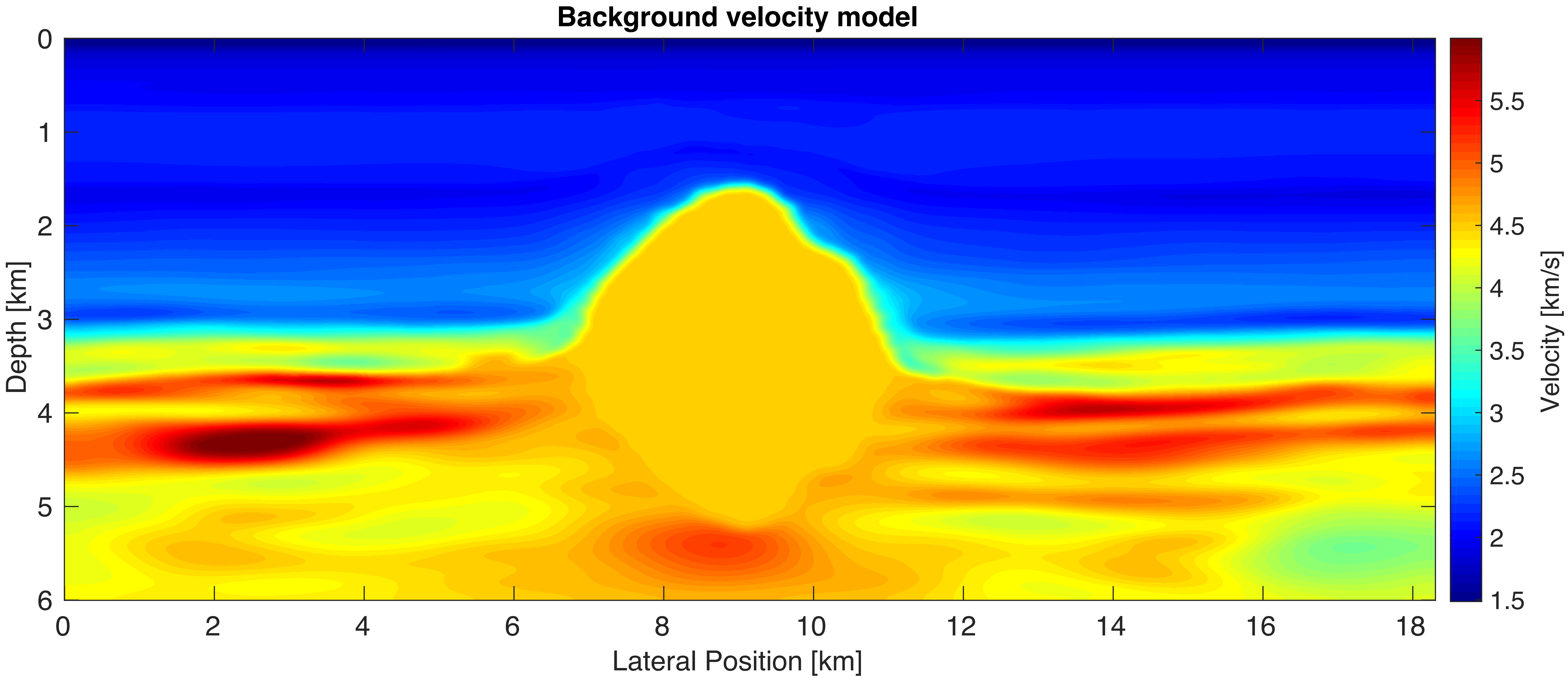

Machar: model parameters

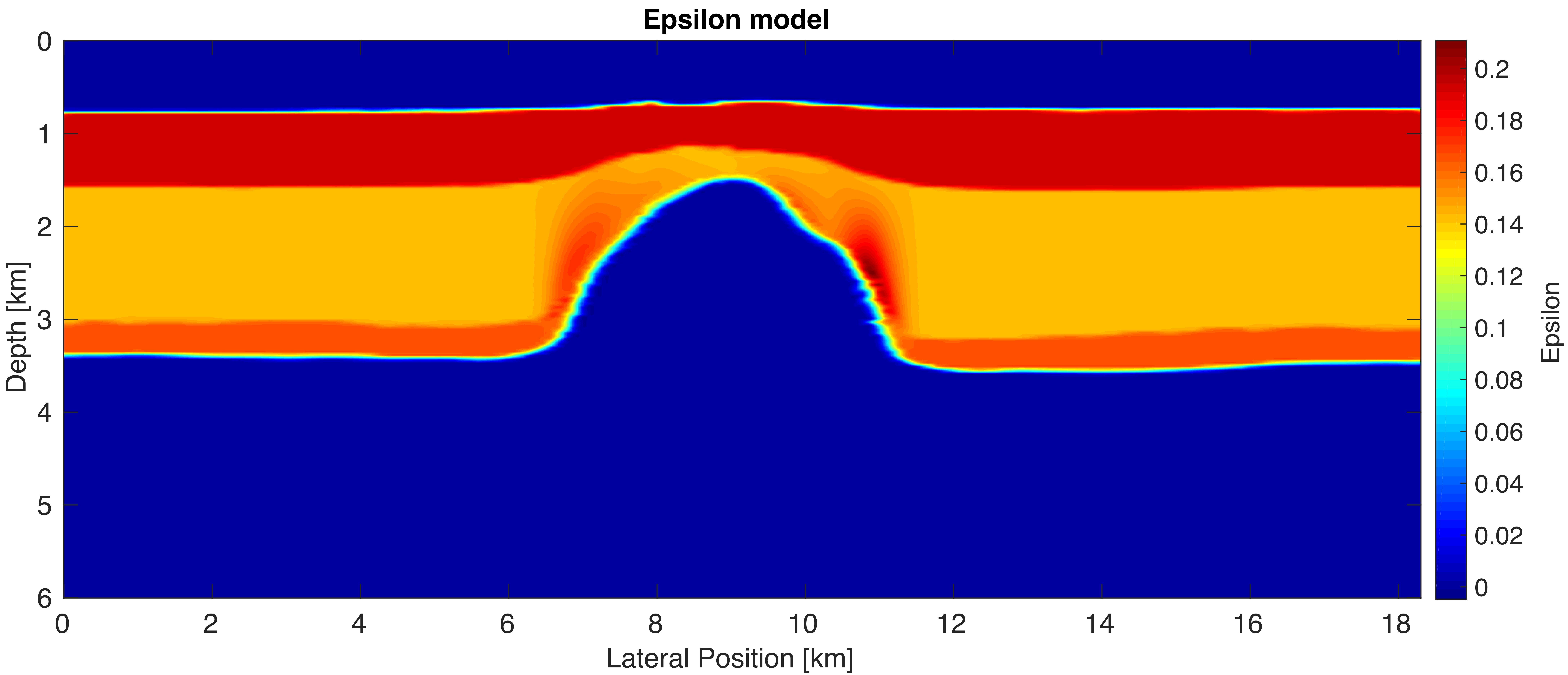

Machar: model parameters

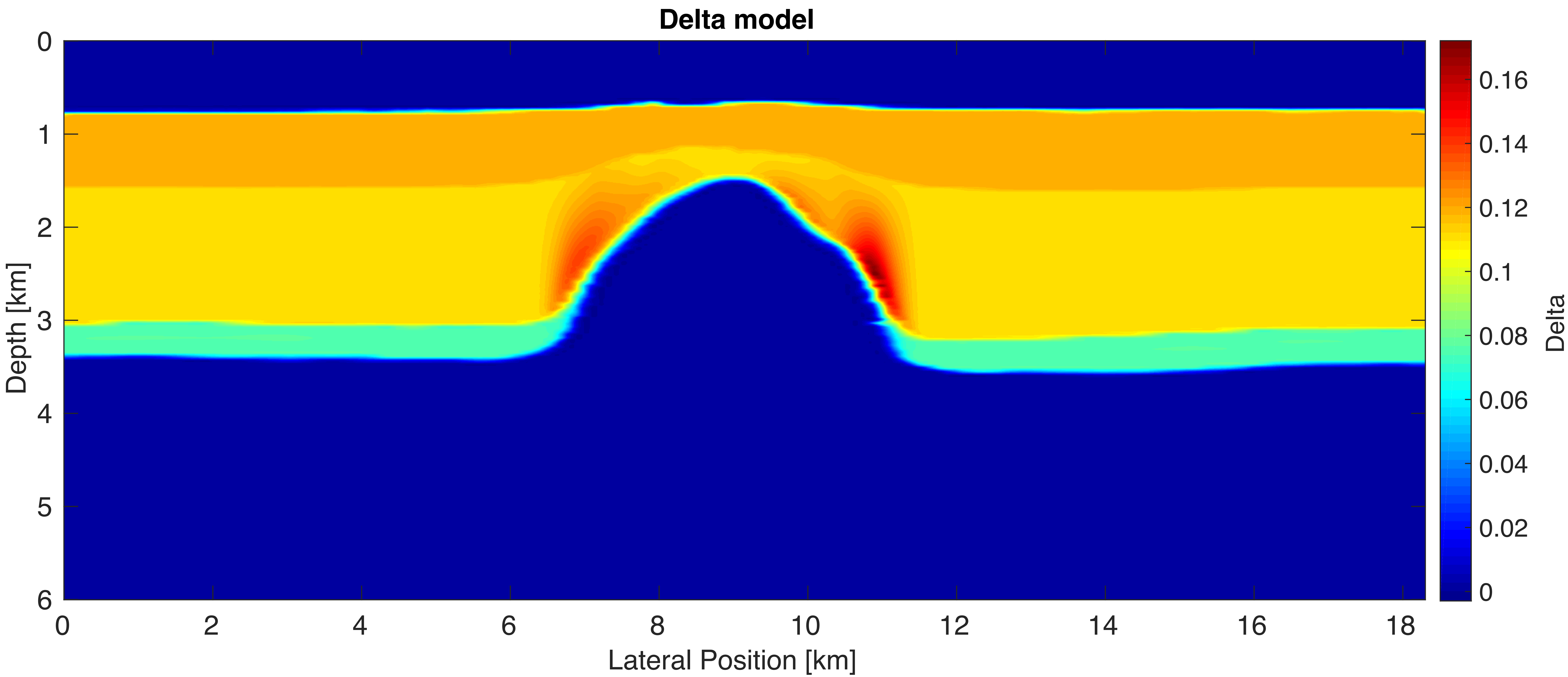

Machar: model parameters

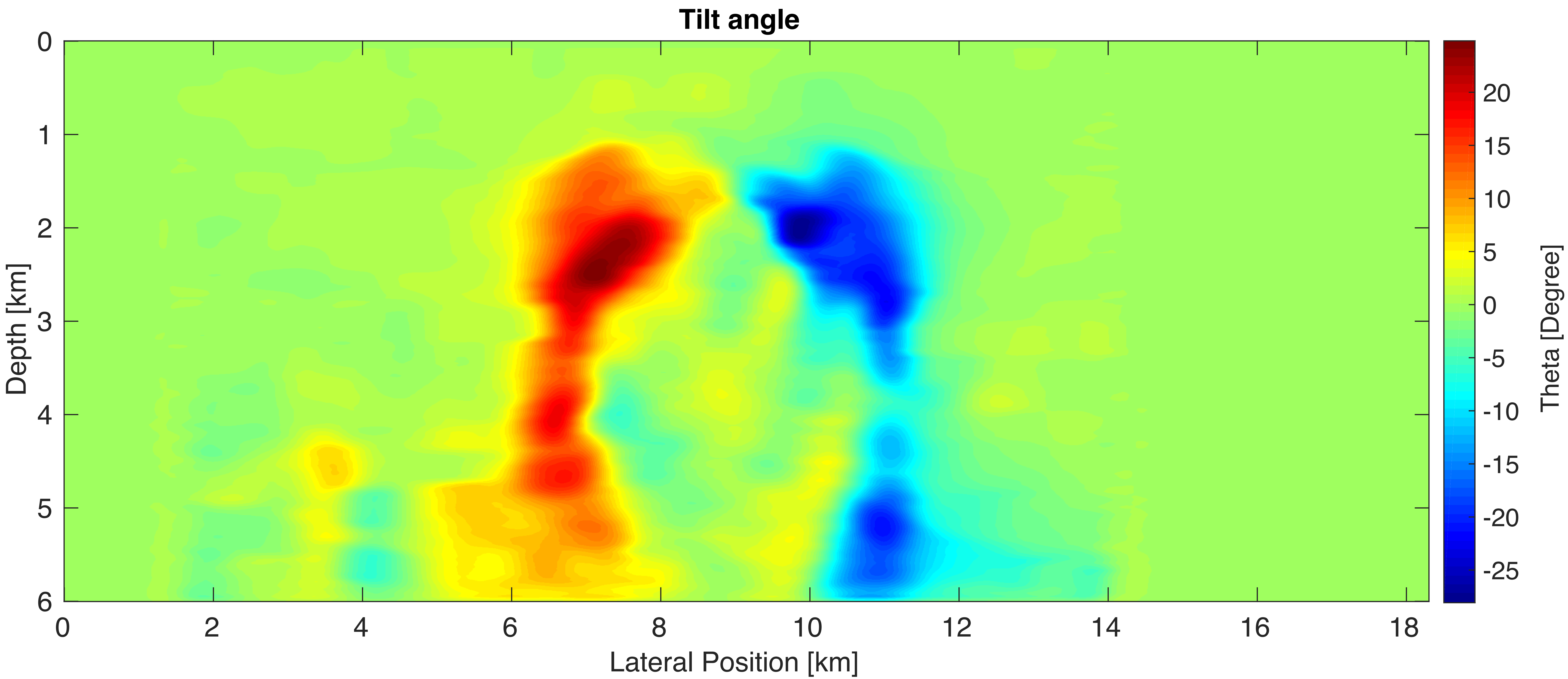

Anisotropic wave equation

2D pure p-wave equation /w PS methods

$$
\begin{aligned}
\frac{\partial U}{\partial t^2} =& c_{xx}\mathcal{F}^{-1}\{-k_x^2\bar{U}\} + c_{zz}\mathcal{F}^{-1}\{-k_z^2\bar{U}\} + c_{xz}\mathcal{F}^{-1}\{-k_xk_z\bar{U}\} \\
&+ c_{xxxx}\mathcal{F}^{-1}\left\{\frac{k_x^4}{k_x^2+k_z^2}\bar{U}\right\} + c_{zzzz}\mathcal{F}^{-1}\left\{\frac{k_z^4}{k_x^2+k_z^2}\bar{U}\right\} \\
&+ c_{xxxz}\mathcal{F}^{-1}\left\{\frac{k_x^3k_z}{k_x^2+k_z^2}\bar{U}\right\} + c_{xzzz}\mathcal{F}^{-1}\left\{\frac{k_xk_z^3}{k_x^2+k_z^2}\bar{U}\right\} \\
&+ c_{xxzz}\mathcal{F}^{-1}\left\{\frac{k_x^2k_z^2}{k_x^2+k_z^2}\bar{U}\right\}
\end{aligned}
$$

k_x: spatial wavenumber in x-direction
$\bar{U}$: wavefield in frequency domain
$\mathcal{F}$: 2D Fourier transform

(Chunlei Chu, Brian K. Macy and Phil D. Anno, 2011)

Reverse time migration

Modeling operator $\mathcal{F}(\mathbf{m})$: generates data $\mathbf{d}$ for model $\mathbf{m}$

($\mathbf{m}$: slowness squared)

Taylor expansion of operator w.r.t. background model $\mathbf{m_0}$

$$\mathcal{F}(\mathbf{m}) = \mathcal{F}(\mathbf{m_0}) + \frac{\partial \mathcal{F}(\mathbf{m_0})}{\partial \mathbf{m}} \delta \mathbf{m} + \mathcal{O}(\delta \mathbf{m}^2)$$

Reverse time migration

Modeling operator $\mathcal{F}(\mathbf{m})$: generates data $\mathbf{d}$ for model $\mathbf{m}$

Taylor expansion of operator w.r.t. background model $\mathbf{m_0}$

$$\mathcal{F}(\mathbf{m}) = \mathcal{F}(\mathbf{m_0}) + \frac{\partial \mathcal{F}(\mathbf{m_0})}{\partial \mathbf{m}} \delta \mathbf{m} + \mathcal{O}(\delta \mathbf{m}^2)$$

observed field data

Reverse time migration

Modeling operator $\mathcal{F}(\mathbf{m})$: generates data $\mathbf{d}$ for model $\mathbf{m}$

Taylor expansion of operator w.r.t. background model $\mathbf{m_0}$

$$\mathcal{F}(\mathbf{m}) = \mathcal{F}(\mathbf{m_0}) + \frac{\partial \mathcal{F}(\mathbf{m_0})}{\partial \mathbf{m}} \delta \mathbf{m} + \mathcal{O}(\delta \mathbf{m}^2)$$

observed field data

modeled data for background model

Reverse time migration

Modeling operator $\mathcal{F}(\mathbf{m})$: generates data $\mathbf{d}$ for model $\mathbf{m}$

Taylor expansion of operator w.r.t. background model $\mathbf{m_0}$

$$\mathcal{F}(\mathbf{m}) = \mathcal{F}(\mathbf{m_0}) + \frac{\partial \mathcal{F}(\mathbf{m_0})}{\partial \mathbf{m}} \delta \mathbf{m} + \mathcal{O}(\delta \mathbf{m}^2)$$

- $\mathcal{F}(\mathbf{m})$: observed field data
- $\mathcal{F}(\mathbf{m_0})$: modeled data for background model
- $\frac{\partial \mathcal{F}(\mathbf{m_0})}{\partial \mathbf{m}}$: Jacobian

Reverse time migration

Modeling operator $\mathcal{F}(\mathbf{m})$: generates data $\mathbf{d}$ for model $\mathbf{m}$

Taylor expansion of operator w.r.t. background model $\mathbf{m_0}$

$$\mathcal{F}(\mathbf{m}) = \mathcal{F}(\mathbf{m_0}) + \frac{\partial \mathcal{F}(\mathbf{m_0})}{\partial \mathbf{m}} \delta \mathbf{m} + \mathcal{O}(\delta \mathbf{m}^2)$$

observed field data — $\mathcal{F}(\mathbf{m})$

modeled data for background model — $\mathcal{F}(\mathbf{m_0})$

seismic image — $\delta \mathbf{m}$

Reverse time migration

Modeling operator $\mathcal{F}(\mathbf{m})$: generates data $\mathbf{d}$ for model

Taylor expansion of operator w.r.t. background model $\mathbf{m_0}$

$$\mathcal{F}(\mathbf{m}) - \mathcal{F}(\mathbf{m_0}) \approx \frac{\partial \mathcal{F}(\mathbf{m_0})}{\partial \mathbf{m}} \delta \mathbf{m} \quad \Longleftrightarrow \quad \delta \mathbf{d} \approx \mathbf{J} \delta \mathbf{m}$$

RTM: apply adjoint Jacobian on data residual: $\delta \mathbf{m} \approx \mathbf{J}^* \delta \mathbf{d}$

Workflow

Anisotropic RTM in time-domain:

- direct backpropagation of input data
- no source estimation (Ricker wavelet at 29 Hz for forward wavefield)
- pure p-wave TTI equation
- grid size of 17 m (3 gridpoints/wavelength)

Plots:

- bandpass filtered images
- depth scaling
- clipped to 97 % of max. amplitudes

Forward Modeling Snapshots

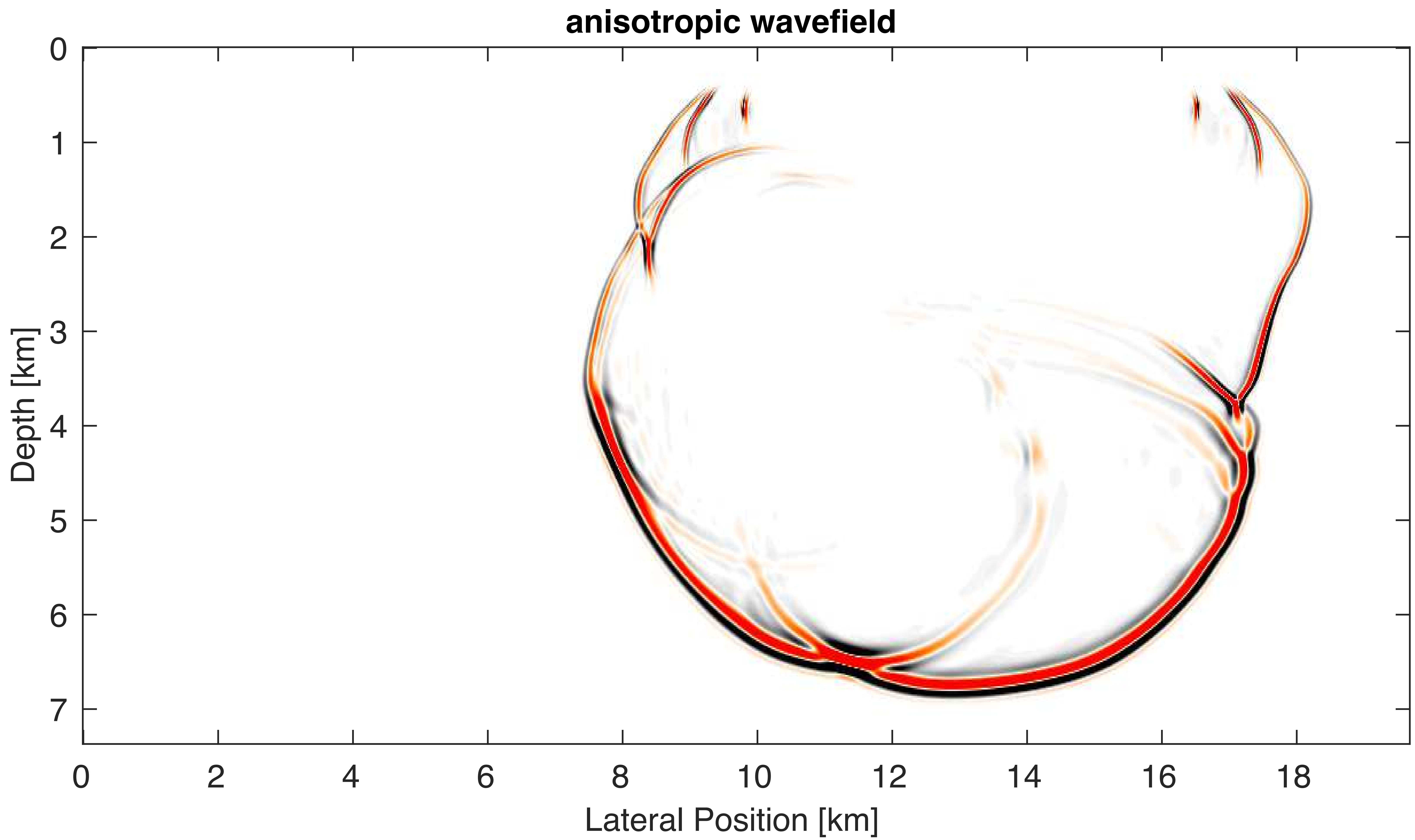

Forward Modeling Snapshots

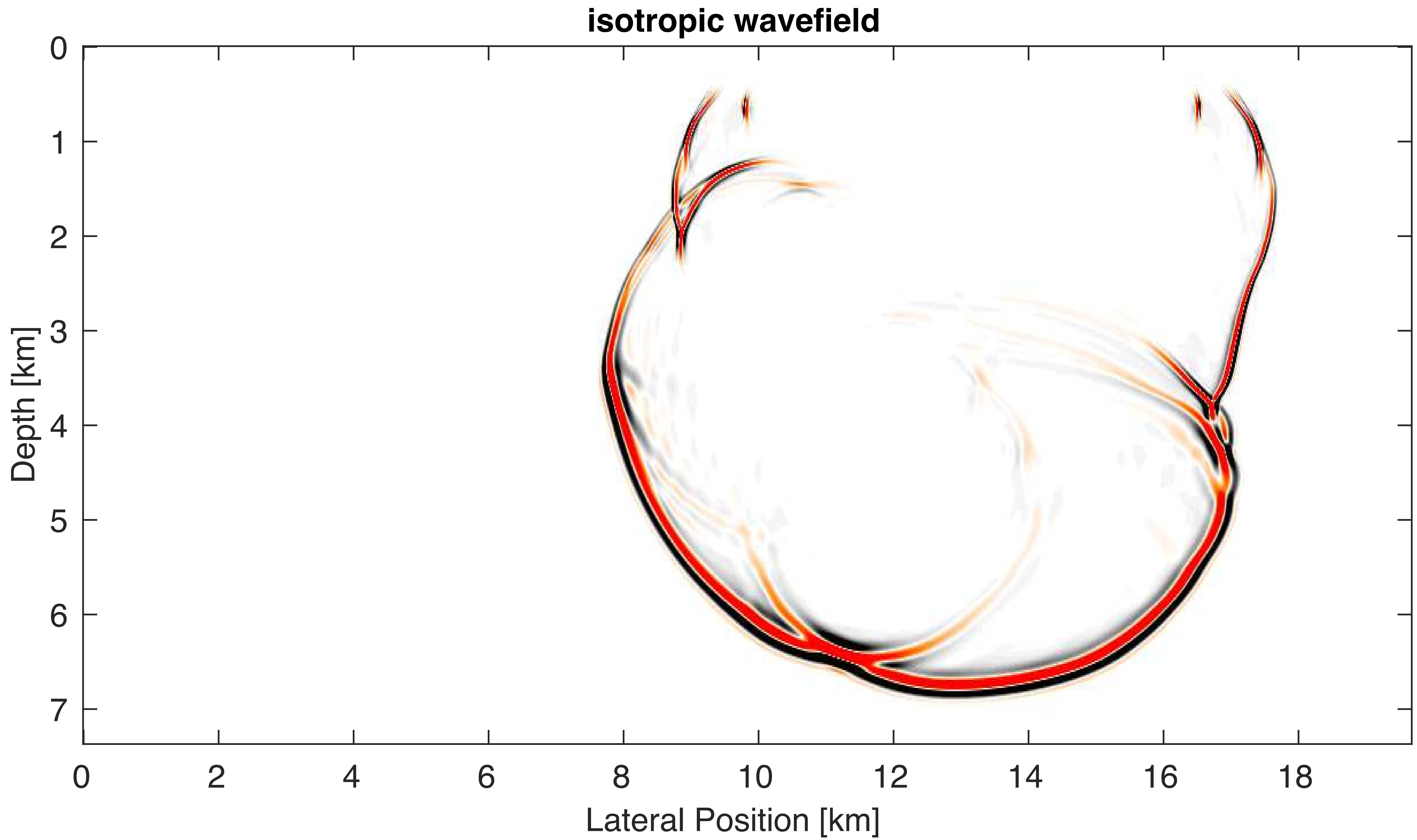

RTM Image

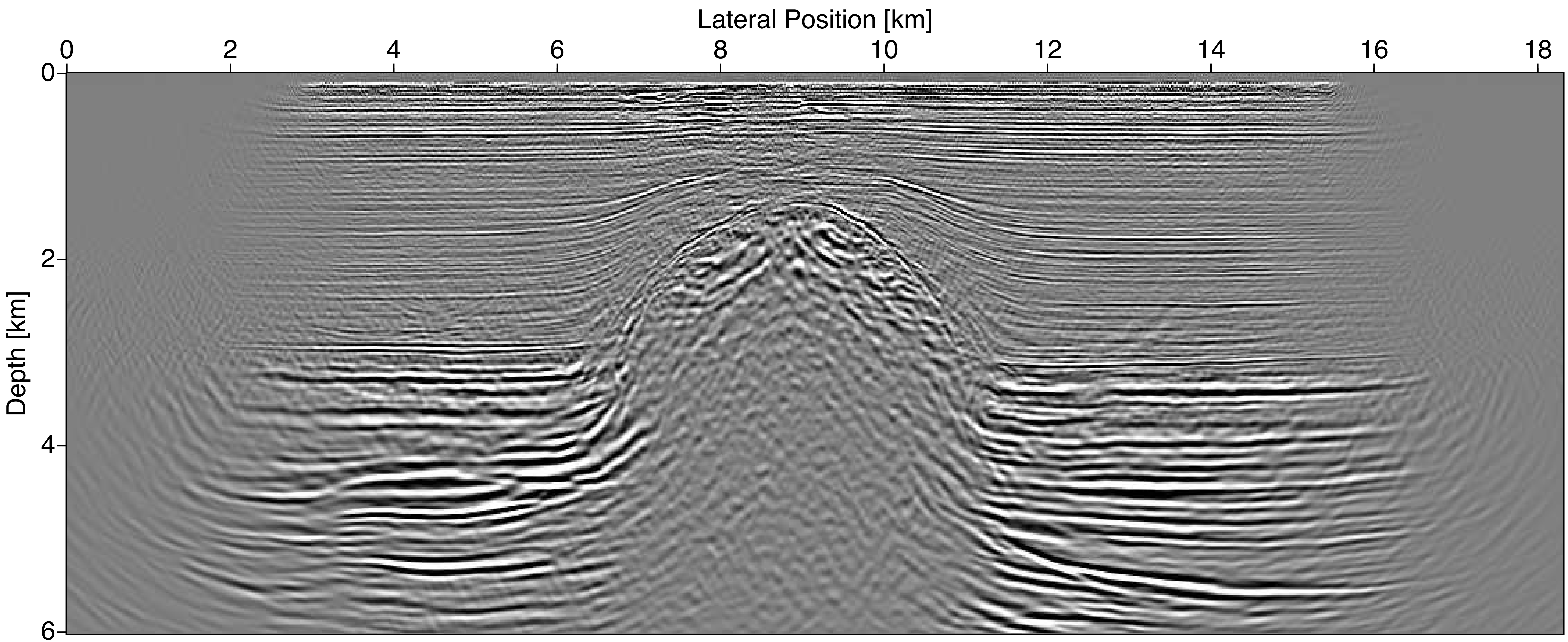

Isotropic RTM

RTM Image

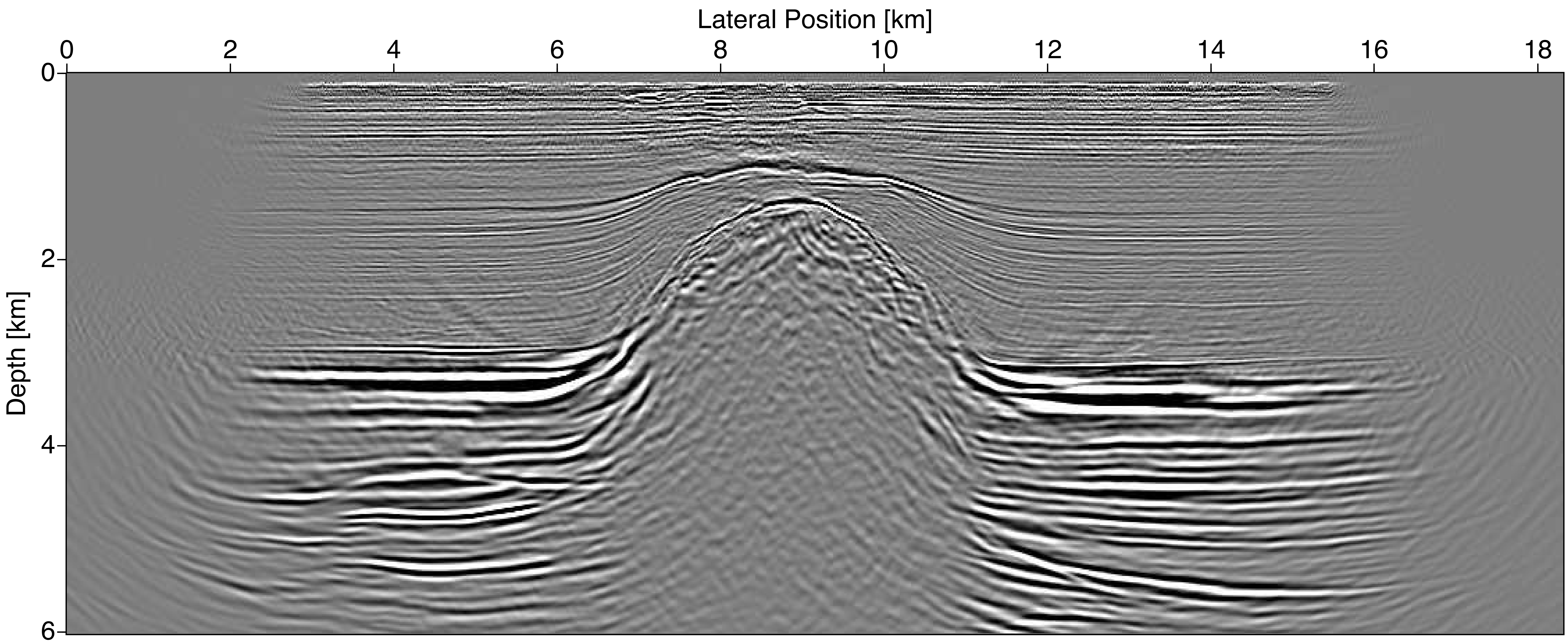

Anisotropic RTM

Close-up

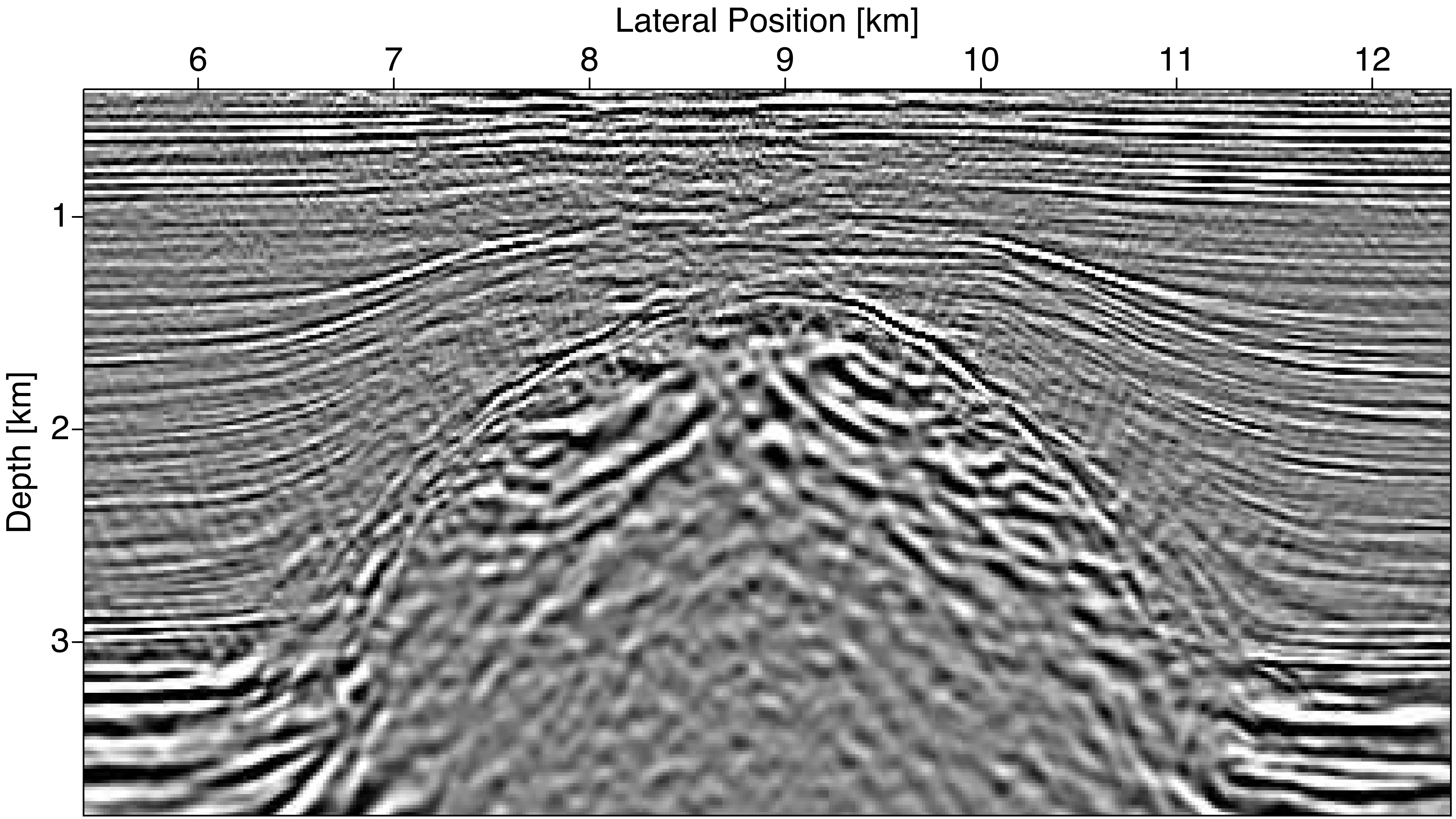

Isotropic RTM

Close-up

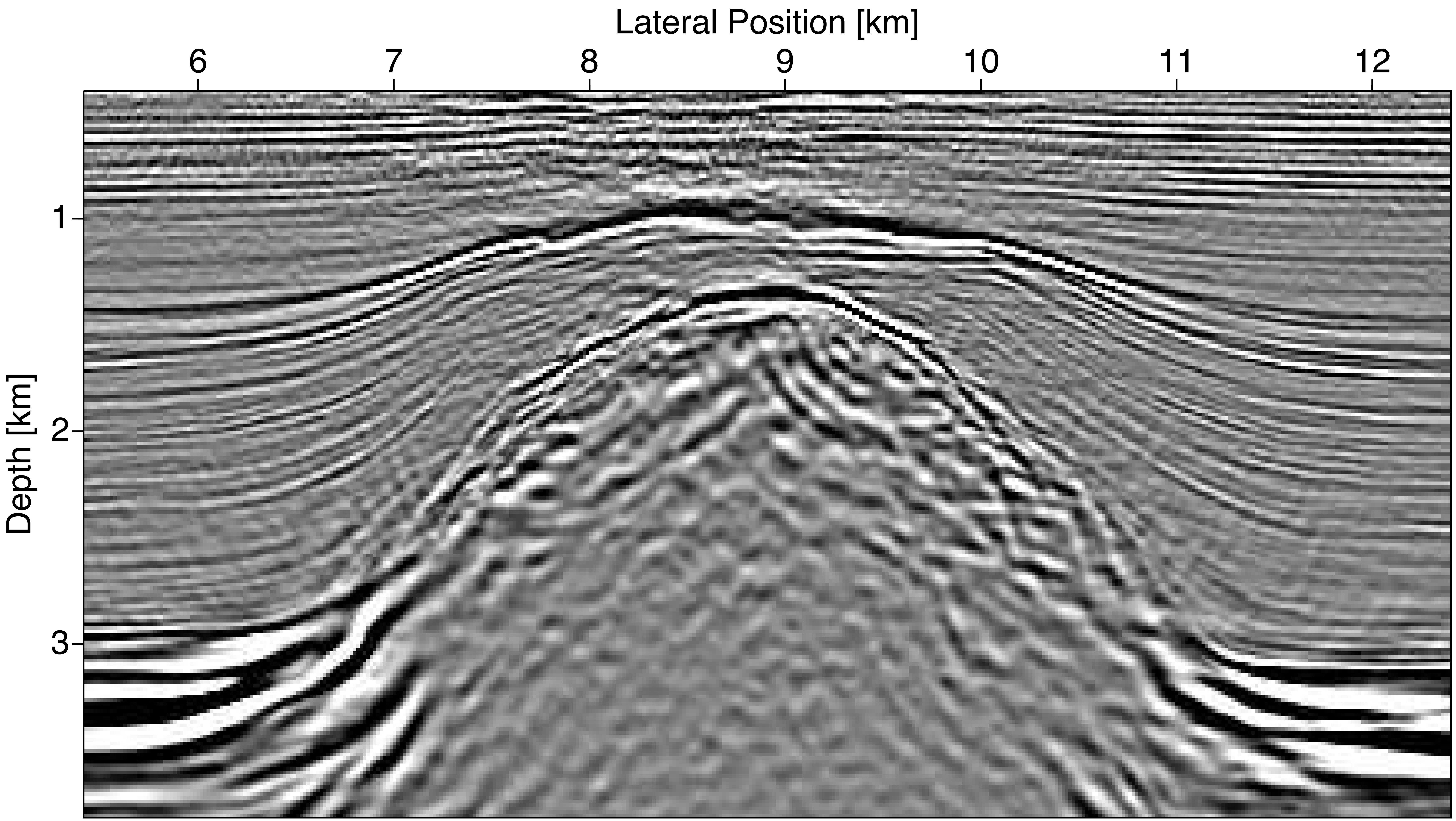

Anisotropic RTM

Close-up

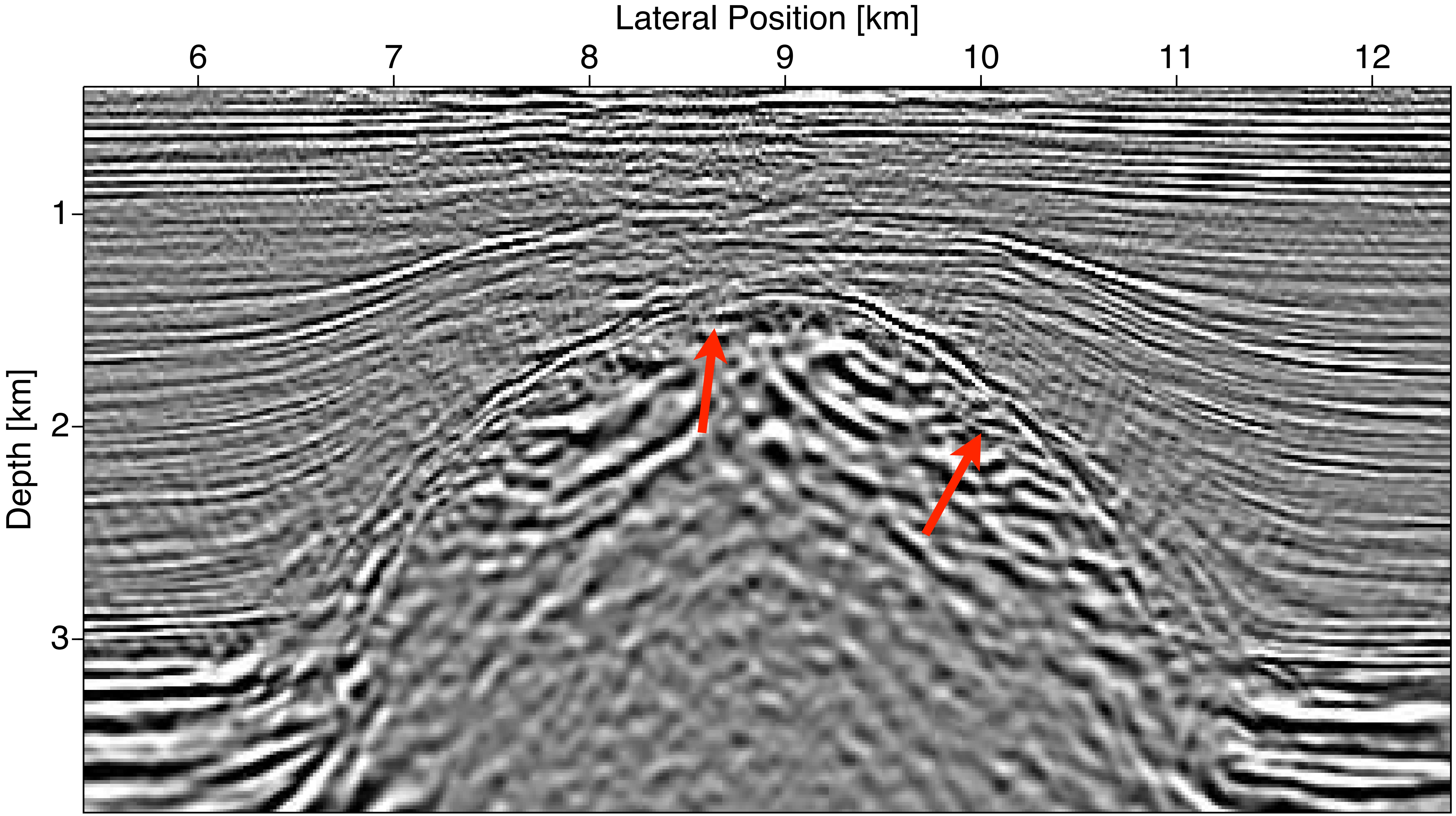

Isotropic RTM

Close-up

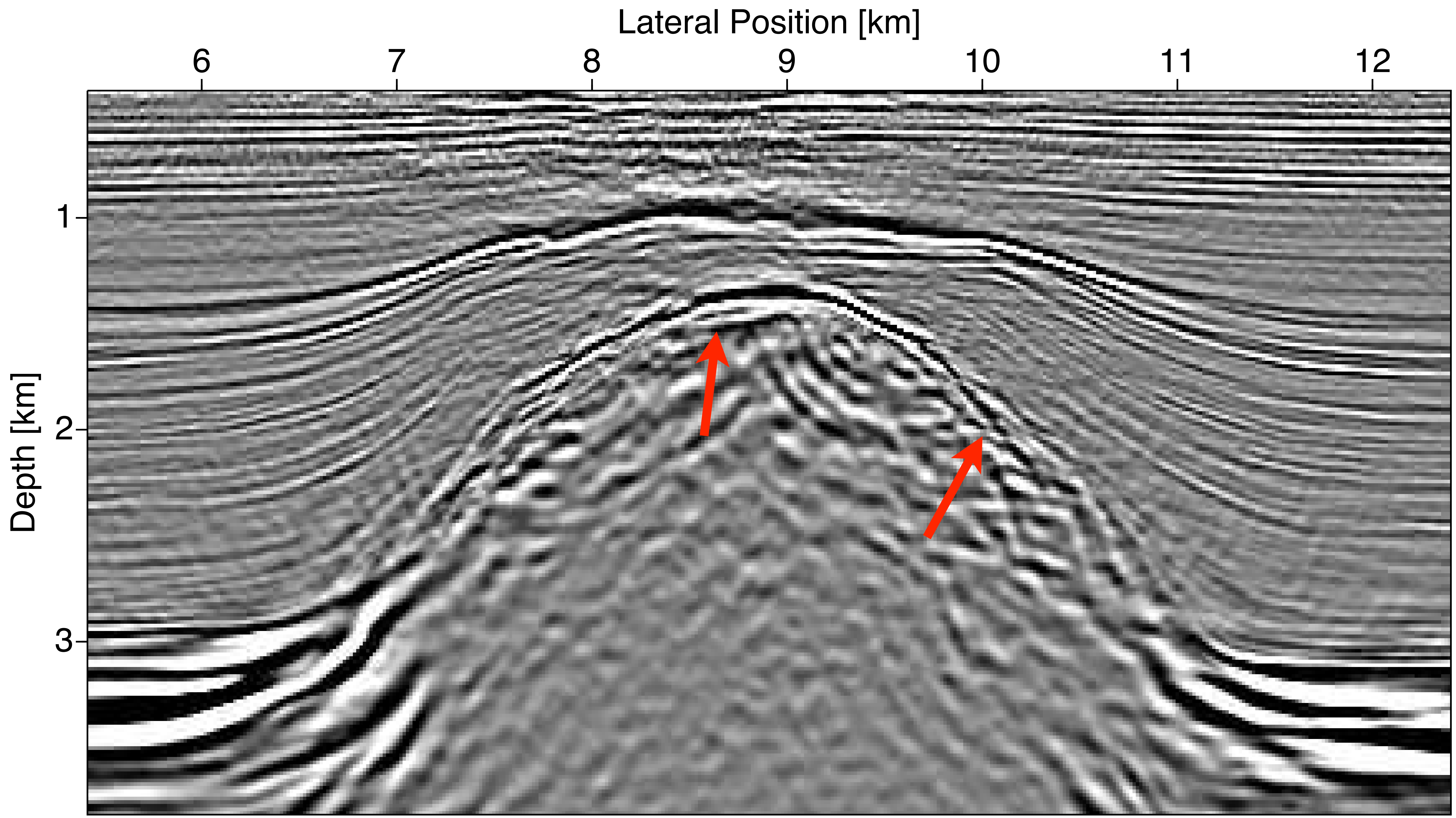

Anisotropic RTM

BP migration results (1989 data set)

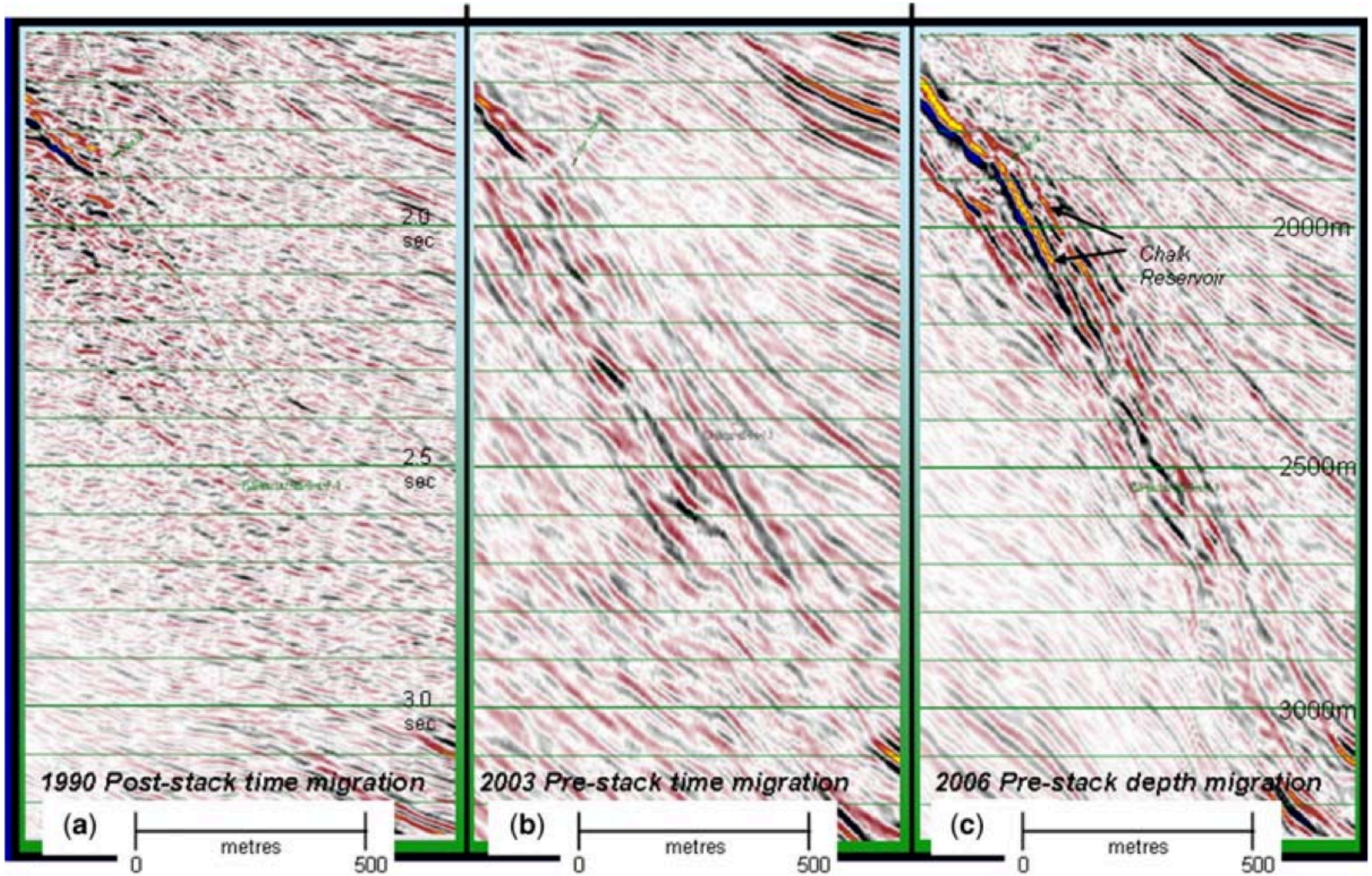

 (Ward et al., 2012, The Machar Oil Field, UK Central North Sea: impact of seismic reprocessing on the development of a complex fractured chalk field)

Close-up

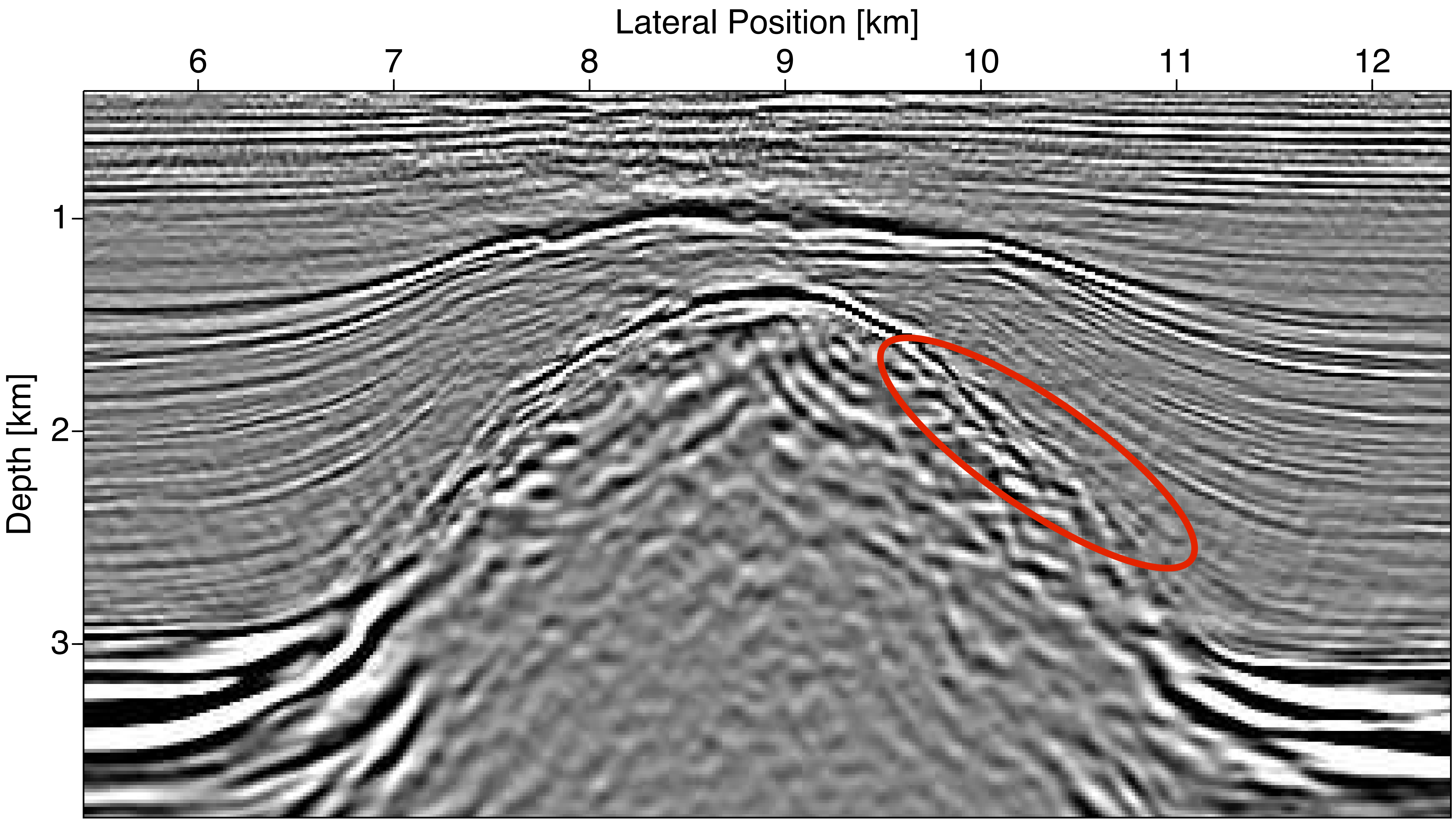

chalk reservoir

Anisotropic RTM

SLIM

Conclusions

RTM with TTI wave equation

- more coherent events in the parts of the model with high anisotropy
- position of salt diapir flanks shifted significantly

Future work

- better strategy to deal with RTM imaging artifacts, alternative imaging condition
- sparsity-promoting least-squares RTM

SLIM

Acknowledgements

Thank you for your attention and thanks to BP for supplying us with this data set!

https://www.slim.eos.ubc.ca

SINBAD

NSERC CRSNG

This work was in part financially supported by the Natural Sciences and Engineering Research Council of Canada Discovery Grant (22R81254) and the Collaborative Research and Development Grant DNOISE II (375142-08). This research was carried out as part of the SINBAD II project with support from the following organizations: BG Group, BGP, CGG, Chevron, ConocoPhillips, ION, Petrobras, PGS, Statoil, Total SA, Sub Salt Solutions, WesternGeco, and Woodside.